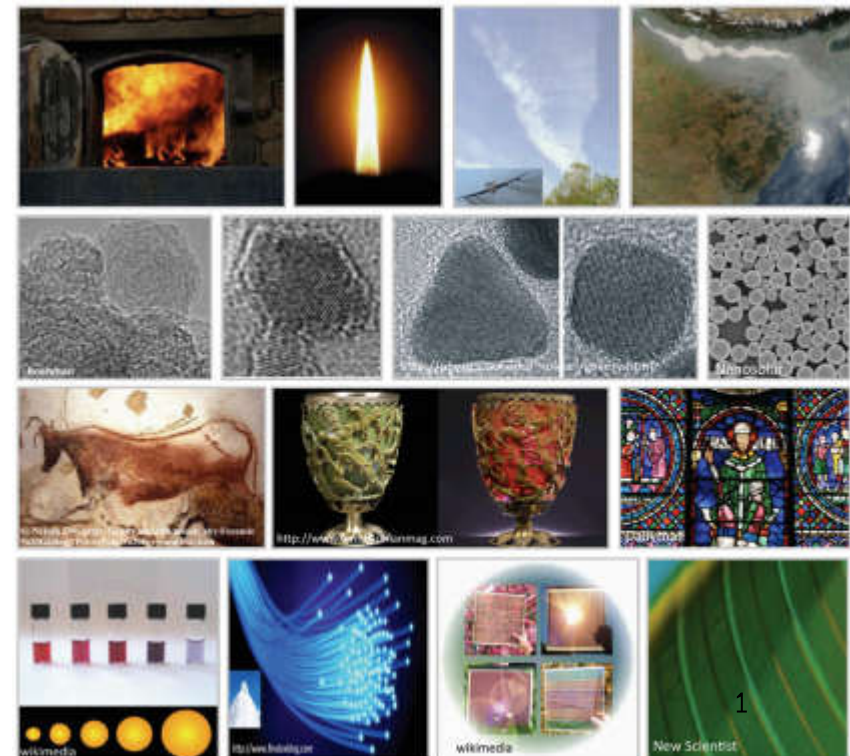


Flame Synthesis of Nanoparticles

Hai Wang
Stanford University



Some Key Papers

1. Ulrich, G.D., 1984. Flame synthesis of fine particles. *Chem. Eng. News* **62**, 22-29.
2. Celii, F.G., Butler, J.E., 1991. Diamond chemical vapor deposition. *Ann. Rev. Phys. Chem.* **42**, pp.643-684.
3. Frenklach, M., Wang, H., 1991. Detailed surface and gas-phase chemical kinetics of diamond deposition. *Phys. Rev. B* **43**, 1520-1545.
4. Brezinsky, K. 1996 Gas-phase combustion synthesis of materials. *Symp. (Int.) Combust.* **26**, 1805-1816.
5. Pratsinis, S.E., 1998. Flame aerosol synthesis of ceramic powders. *Prog. Energy Combust. Sci.* **24**, pp.197-219.
6. Wooldridge, M.S., 1998. Gas-phase combustion synthesis of particles. *Progress in Energy and Combustion Science*, **24**, 63-87.
7. Kammler, H.K., Mädler, L. and Pratsinis, S.E., 2001. Flame synthesis of nanoparticles. *Chem. Eng. Technol.* **24**, 583-596.
8. Height, M.J., Howard, J.B., Tester, J.W. and Vander Sande, J.B., 2004. Flame synthesis of single-walled carbon nanotubes. *Carbon*, **42**, 2295-2307..
9. Roth, P., 2007. Particle synthesis in flames. *Proc. Combust. Inst.* **31**, 1773-1788.
10. Li, S., Ren, Y., Biswas, P. and Tse, S. D., 2016. Flame aerosol synthesis of nanostructured materials and functional devices: Processing, modeling, and diagnostics. *Prog. Energy Combust. Sci.* **55**, 1-59.
11. Kelesidis, G.A., Goudeli, E. and Pratsinis, S.E., 2017. Flame synthesis of functional nanostructured materials and devices: Surface growth and aggregation. *Proc. Combust. Inst.* **36**, 29-50.



Outline

- 1. A brief history about earlier applications of nanoparticles**
2. Modern applications of nanoparticles: why are they fascinating?
3. Industrial-scale combustion synthesis
4. Thermodynamics again
5. Brief overview of synthesis flames and processes
6. Several case studies
 - “infant” soot as a quantum dot/fluorescent material
 - Titania as an electron transfer media and sensor material
 - Control titania crystal phase using flame stoichiometry

Nanoparticles have a long history



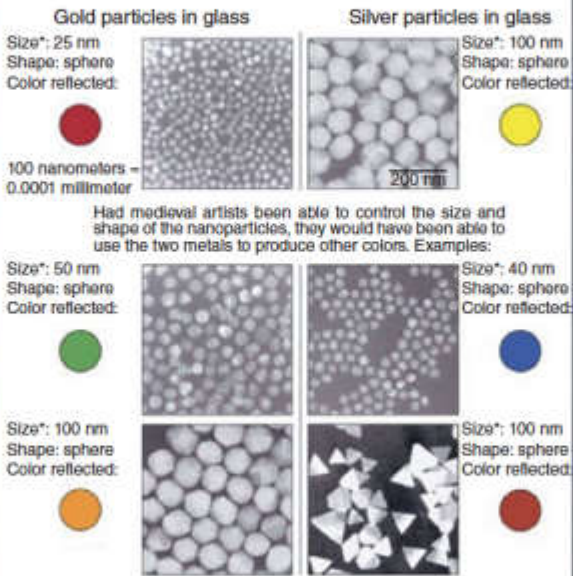
This 1,600-Year-Old Goblet shows that the Romans were Nanotechnology Pioneers

<http://www.smithsonianmag.com/history-archaeology/This-1600-Year-Old-Goblet-Shows-that-the-Romans-Were-Nanotechnology-Pioneers-220563661.html#ixzz2pdrVS5WI>



The First Nanotechnologists

Ancient stained-glass makers knew that by putting varying, tiny amounts of gold and silver in the glass, they could produce the red and yellow found in stained-glass windows. Similarly, today's scientists and engineers have found that it takes only small amounts of a nanoparticle, precisely placed, to change a material's physical properties.



Source: © Chad A. Mirkin, Institute of Nanotechnology, Northwestern University

*Approximate



Outline

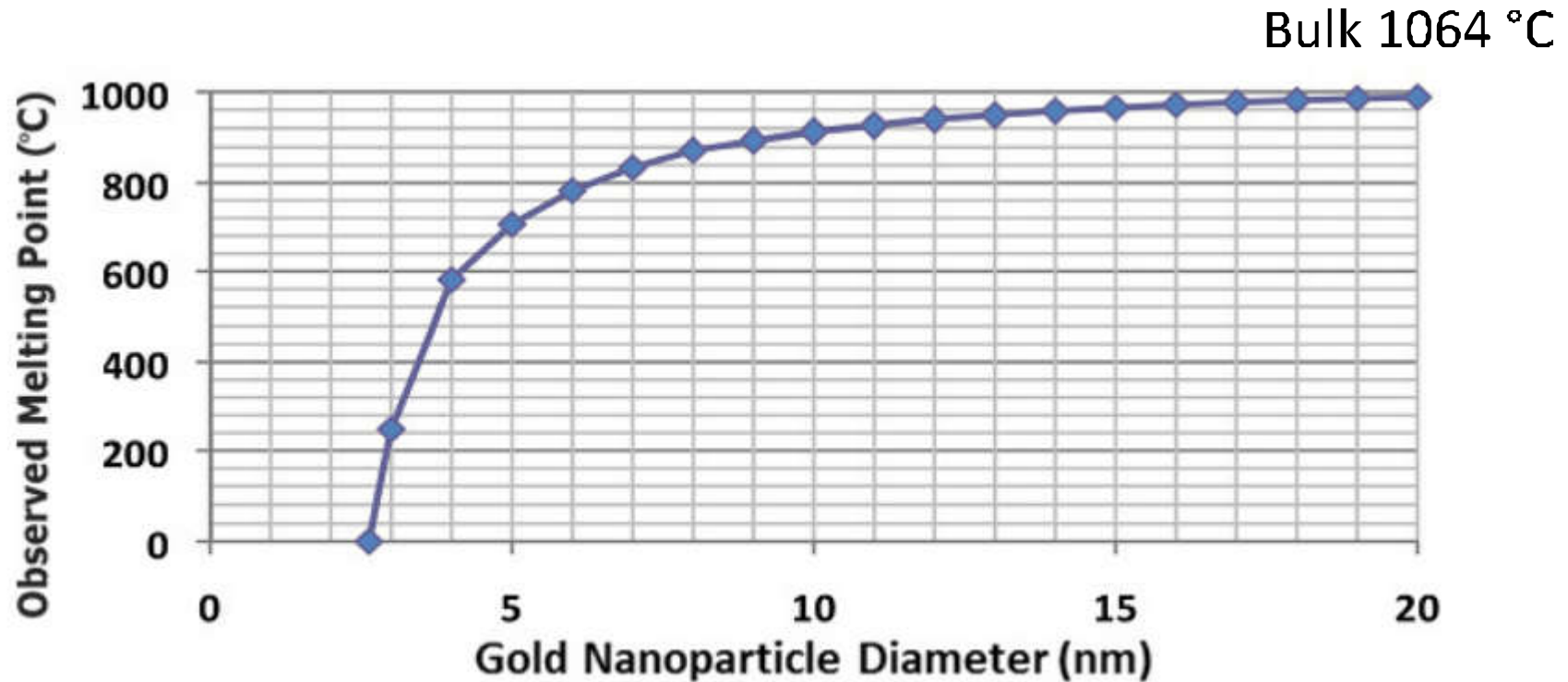
1. A brief history about earlier applications of nanoparticles
- 2. Modern applications of nanoparticles: why are they fascinating?**
3. Industrial-scale combustion synthesis
4. Thermodynamics again
5. Brief overview of synthesis flames and processes
6. Several case studies
 - “infant” soot as a quantum dot/fluorescent material
 - Titania as an electron transfer media and sensor material
 - Control titania crystal phase using flame stoichiometry

Principle Properties of Nanoparticles and Their Variations

- Size and its distribution
- Specific surface area
- Shape and morphology
- Morphology and aggregation
- Composition (surface versus interior, surface modification)
- Fluid media
 - Aerosol—Solid or liquid matters in a gas
 - Suspension—Solid in liquids
 - Emulsion—two liquid phases
- Phase transition
- Light absorption/scattering/emission
- Band gap and quantum confinement
- Magnetic properties
- Electric charging, ionization potential
- Interactions among themselves – coagulation & aggregation
- Interactions with gas – adsorption & reaction

How materials change themselves at nanoscales?

Example 1: Phase Transition



G. Schmid and B. Corain, "Nanoparticulated Gold: Syntheses, Structures, Electronics, and Reactivities," *European Journal of Inorganic Chemistry* 17 (2003) 3081–3098.

How materials change themselves at nanoscales?

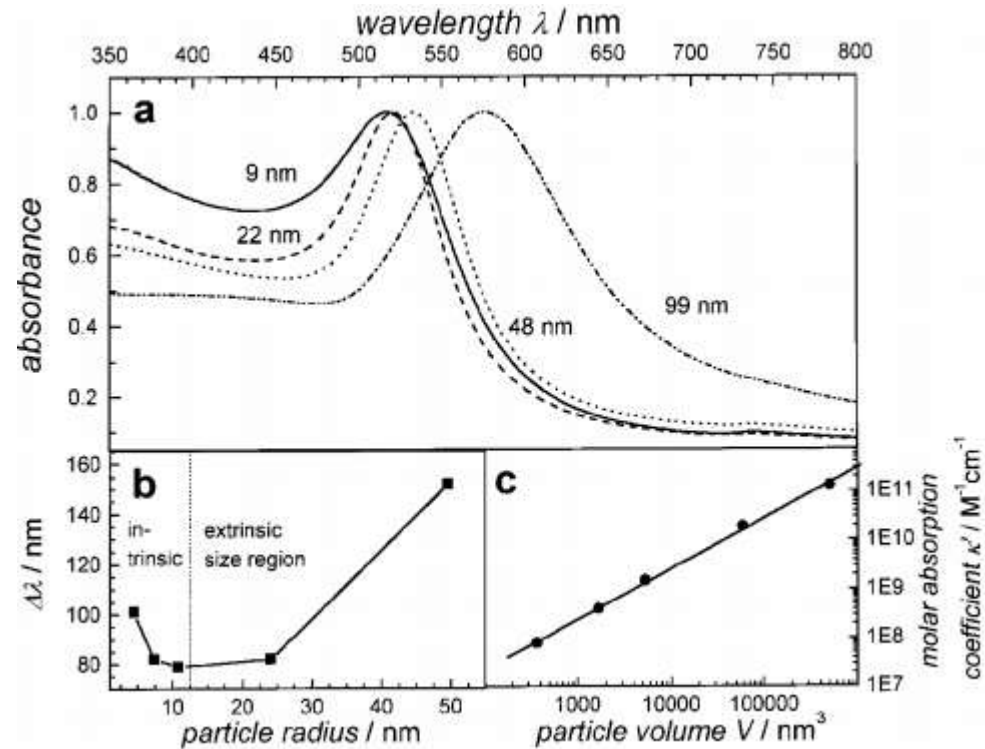
Example 2: Optical Properties



Gold and silver nanoparticles of varying sizes and shapes. From left to right:

- 80 nm silver spheres
- 20 nm silver spheres
- 40 nm gold spheres
- 12 nm gold spheres
- 200 nm silver plates
- 120 nm silver plates
- 60 nm silver plates

(<http://nanocomposix.com/kb/general/color-engineering>)



S. Link, M. A. El-Sayed, *J. Phys. Chem. B* 103 (1999) 8410-8426.

A surface plasmonic resonance effect: the interaction of light with surface conduction electrons

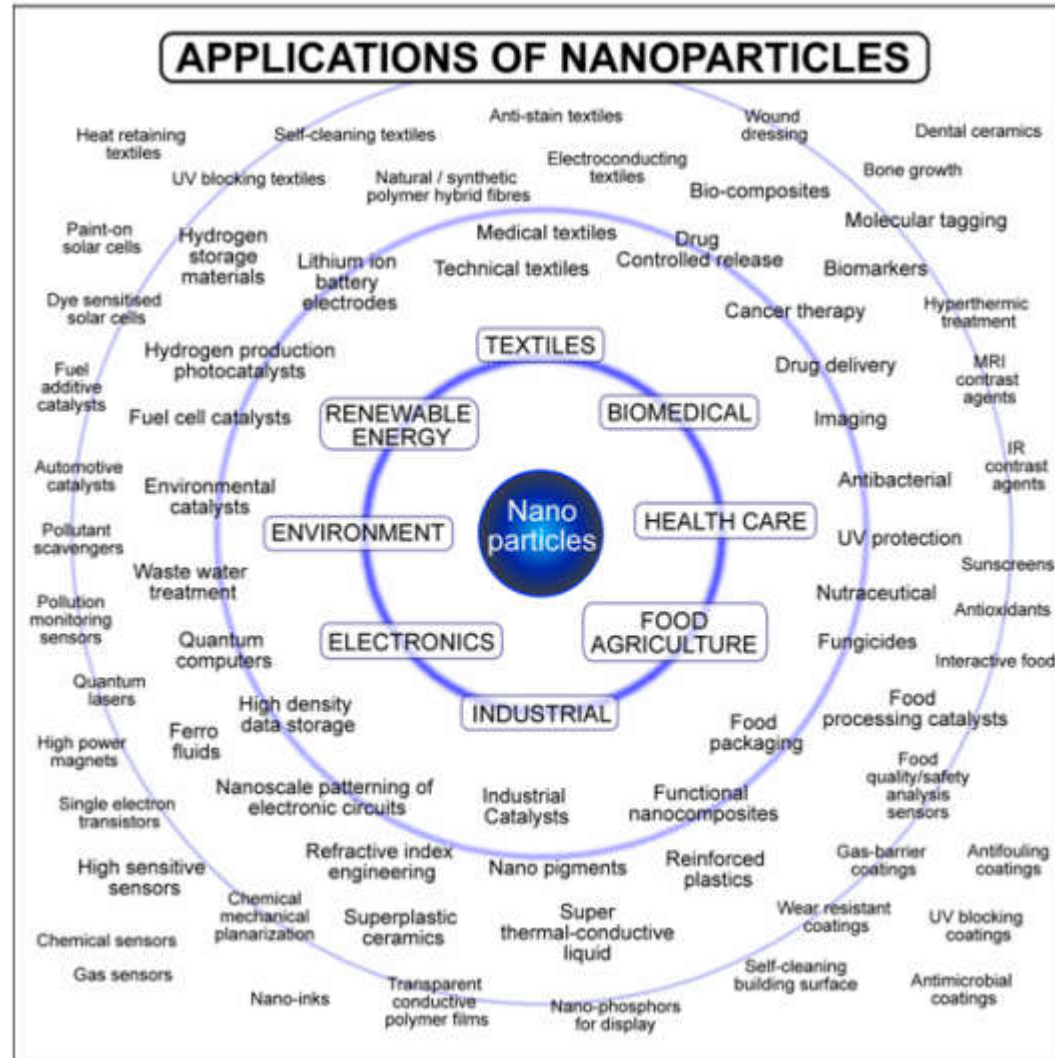
Why Nanoparticles?

A fascinating, developing science

- Wanted versus unwanted
 - Wanted: useful materials
 - Unwanted: particulate pollutants, particle induced super knock in engines etc
- Small versus large;
- From one crystal phase to another
- Single versus multicomponent composition and phases;
- Low to high dimensions;
- Wide ranging properties of light interactions;
- From old to new energy sciences and devices

Why Nanoparticles?

- In Nanotechnology and materials application



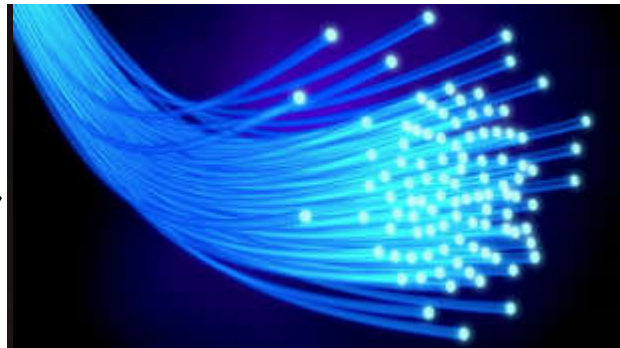
Why Nanoparticles?

Paint pigments and fibre optics

Titania
 TiO_2



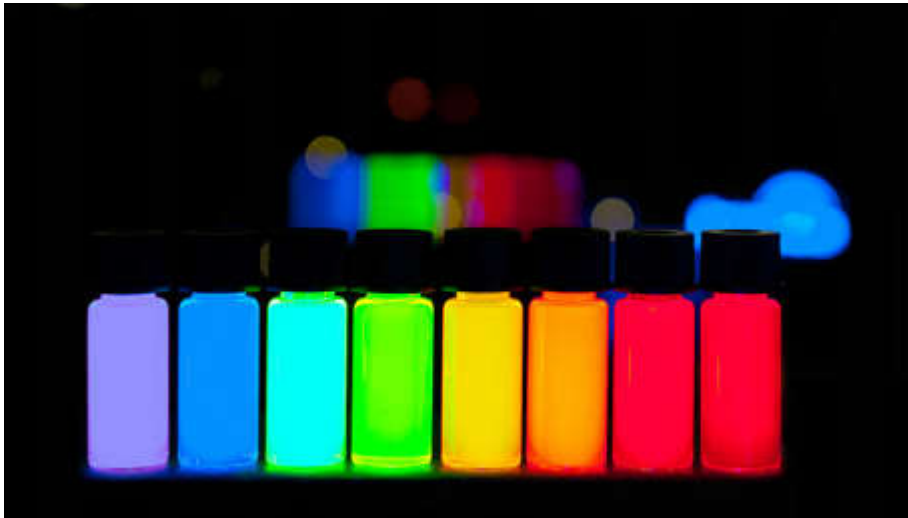
Silicate
 SiO_2



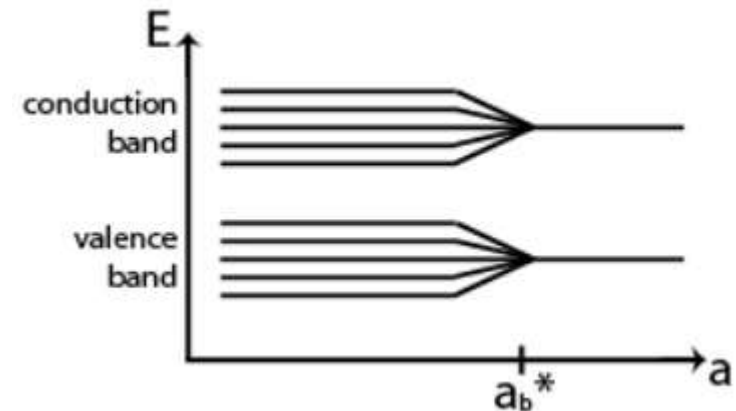
Why Nanoparticles?

Quantum dot and photonics

Fluorescence of semiconductor nanoparticles under UV



wikimedia

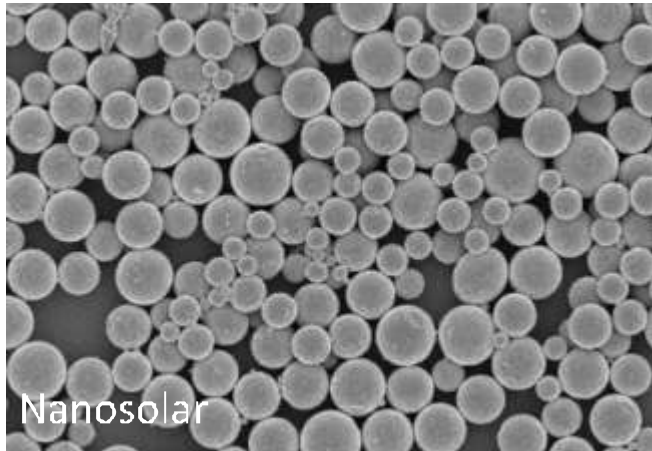


Splitting of energy levels for small quantum dots due to the quantum confinement effect. The horizontal axis is the radius, or the size, of the quantum dots and a_b^* is the Exciton Bohr radius

Why Nanoparticles?

Photovoltaics and Solar Cells

Flexible solar cells



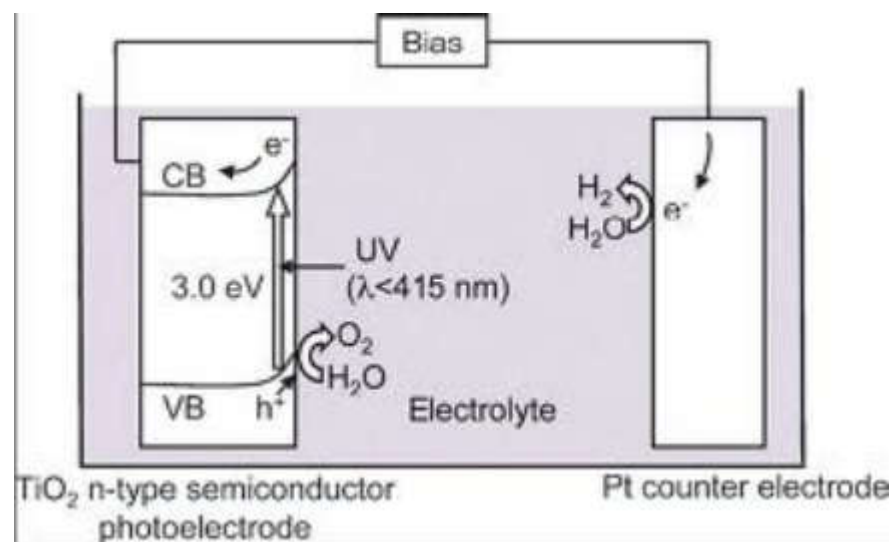
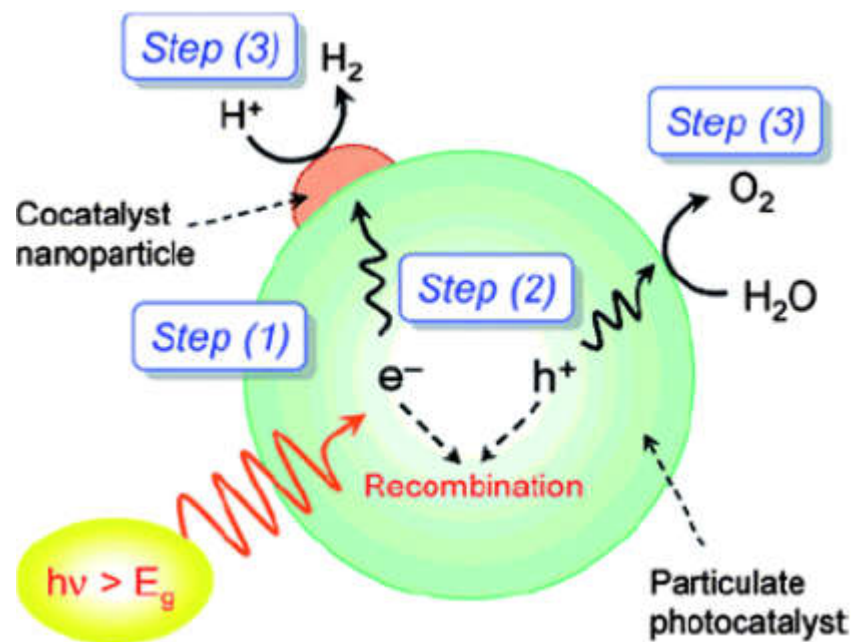
Dye sensitized solar cells



New Scientist, April 10th, 2010.

Why Nanoparticles?

Photocatalytic water splitting

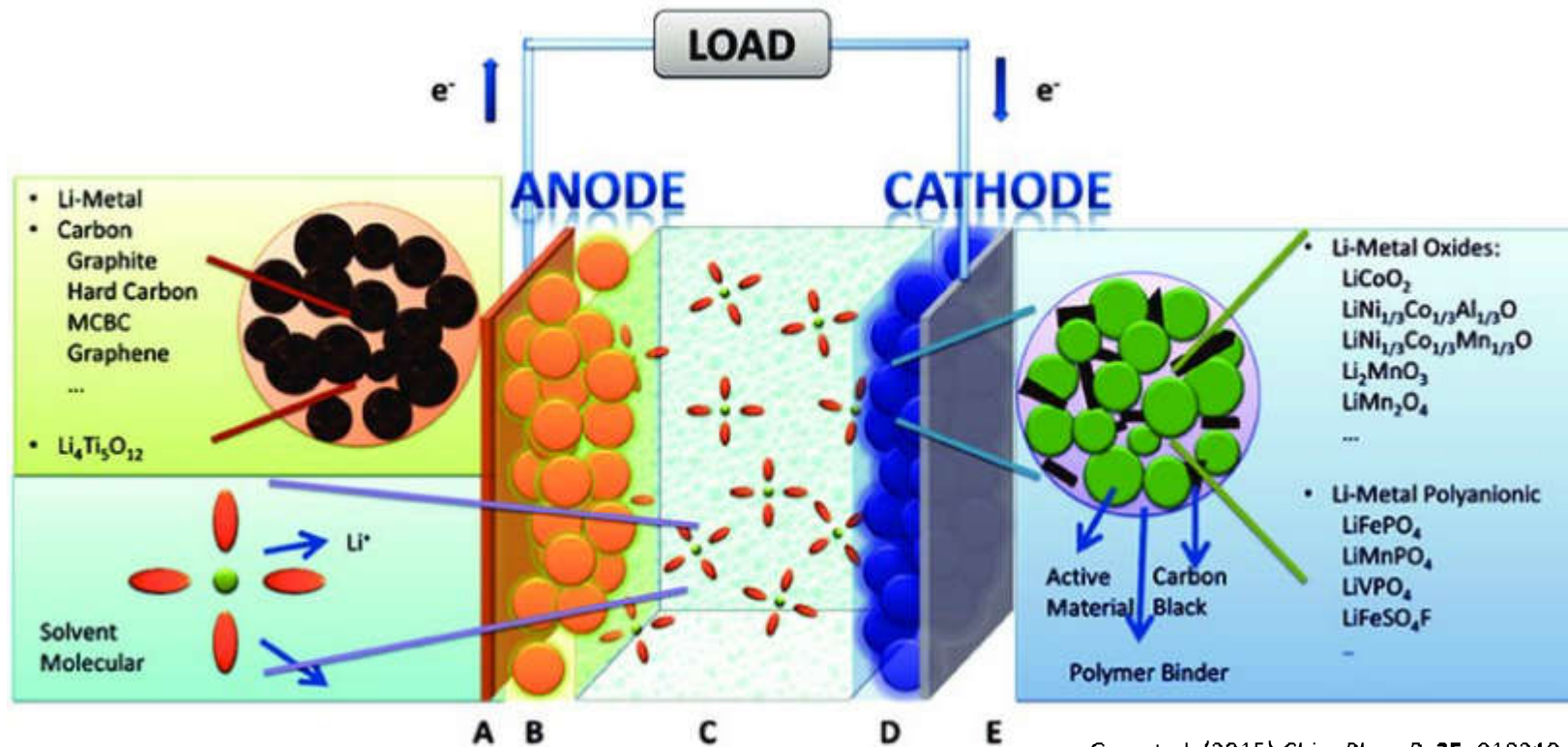


Honda-Fujishima effect

M. Kitano, M. Hara *J. Mater. Chem.*, 2010, 20, 627-641

Why Nanoparticles?

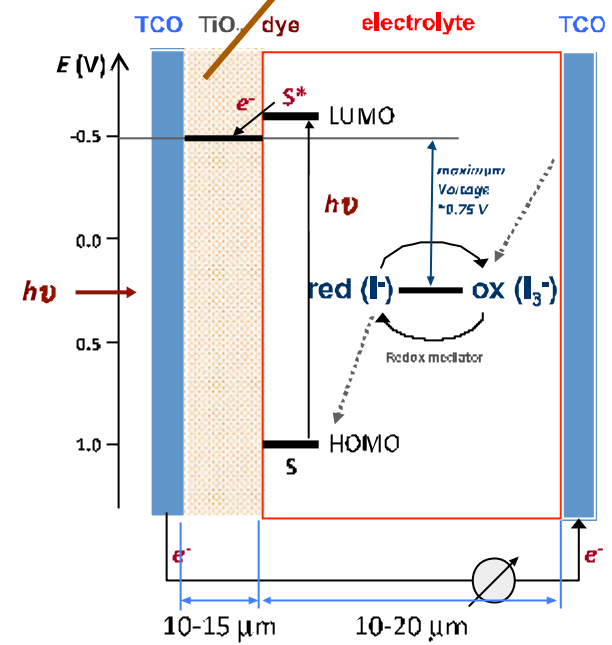
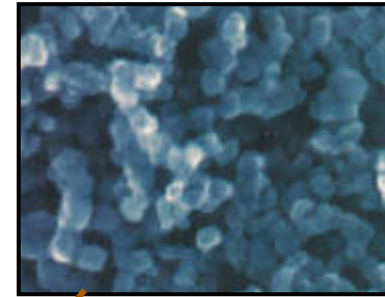
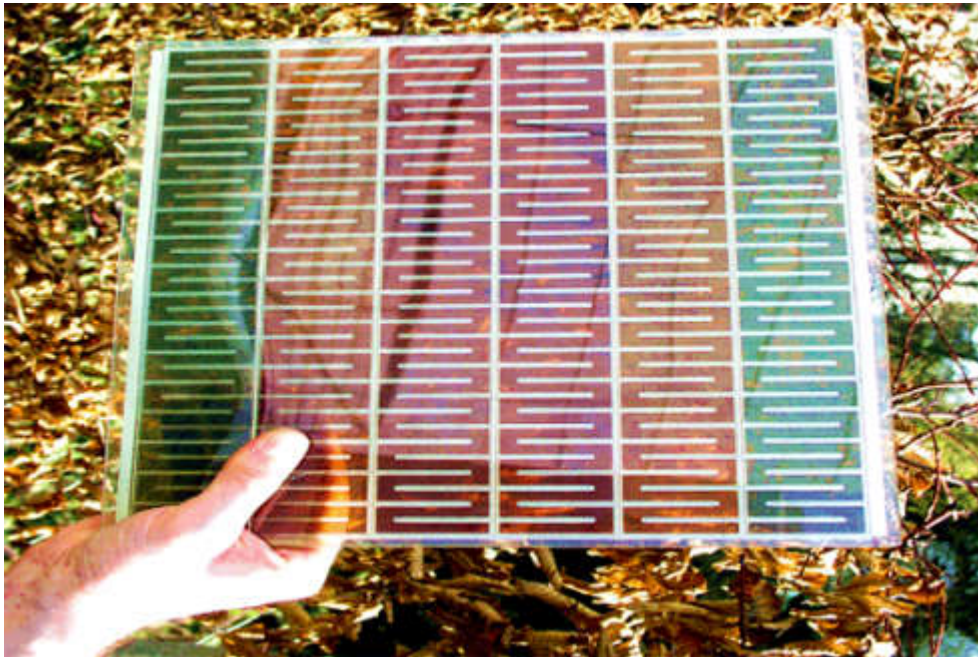
Lithium ion and other rechargeable batteries



Gao et al. (2015) *Chin. Phys. B*, **25**, 018210.

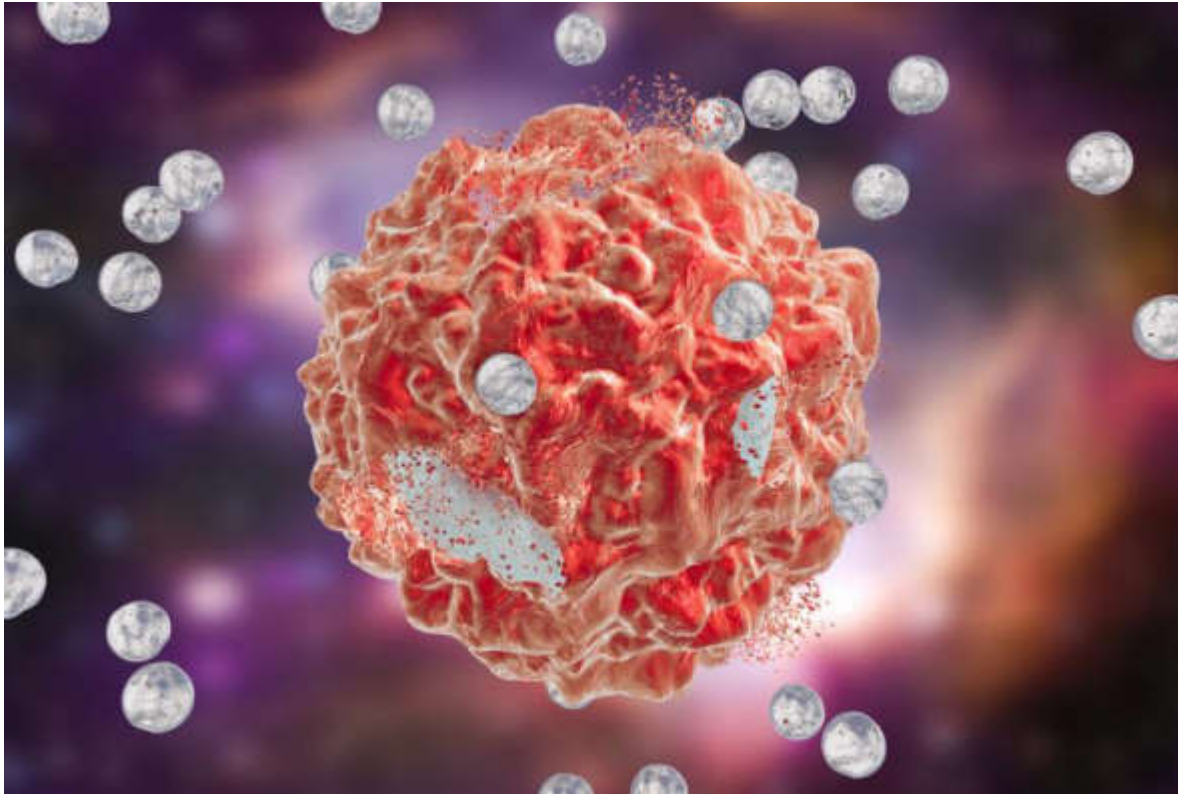
Why Nanoparticles?

Dye-Sensitized Solar Cell



Why Nanoparticles?

Medicine: cancer treatment



Nanoparticles injected into the tumor produce heat by applying magnetic fields, X-Rays or light, thus destroy cancer cells

Encapsulation of chemotherapy drugs allows localized delivery (reduced toxicity)

<https://www.rdmag.com/article/2018/02/nanoparticle-based-cancer-treatment-look-its-origins-and-whats-next>

Studies of Nanoparticles

- **An interdisciplinary science**
 - Chemistry (composition, reactivity, kinetics)
 - Physics (quantum effects, magnetism)
 - Engineering (transport, characterization, fabrication)
- **With exceedingly broad applications**
 - Nearly all (new and old) energy conversion processes
 - Air pollution/climate change
 - Medicine

Outline

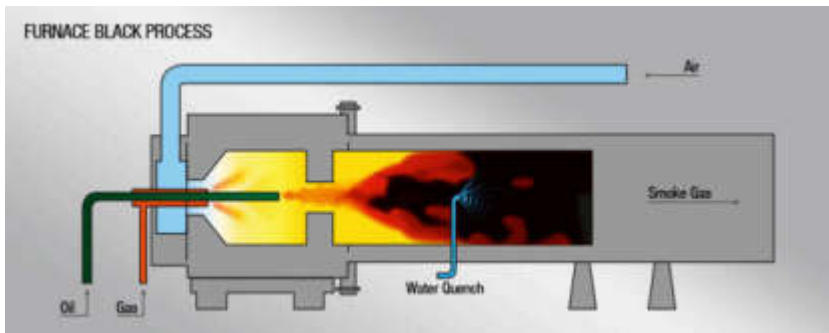
1. A brief history about earlier applications of nanoparticles
2. Modern applications of nanoparticles: why are they fascinating?
- 3. Industrial-scale combustion synthesis**
4. Thermodynamics again
5. Brief overview of synthesis flames and processes
6. Several case studies
 - “infant” soot as a quantum dot/fluorescent material
 - Titania as an electron transfer media and sensor material
 - Control titania crystal phase using flame stoichiometry

Flame Synthesis of Nanoparticles - Advantages

- Material and phase purity
- Good size control
- Scalable, and cost effective
- Versatile in the type of materials that can be synthesized
- Can combine synthesis with device fabrication in a single step
- Open-air reel-to-reel processing possible

Combustion Synthesis – Traditional Materials

Carbon black



<https://pentacarbon.de/en/wiki/>



<http://www.waymarking.com/gallery/image.aspx?f=1&guid=d10bb784-971a-4781-81cf-281332121cbd>

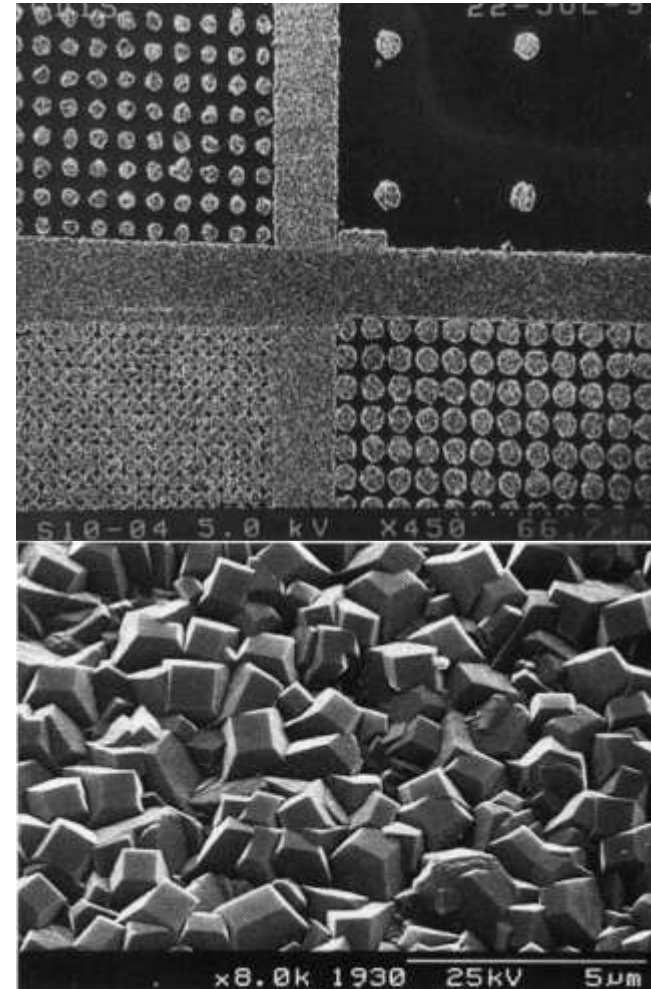
Diamond CVD using Oxyacetylene Torch



<https://www.pinterest.co.uk/pin/85061042851322893/>

Applications:

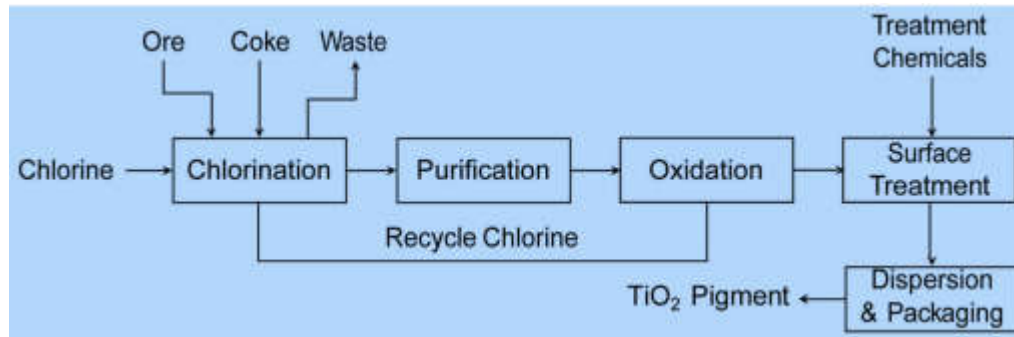
- X-ray detector windows
- Abrasives
- Electronic packaging
- IR optical coatings
- Machine tool coatings



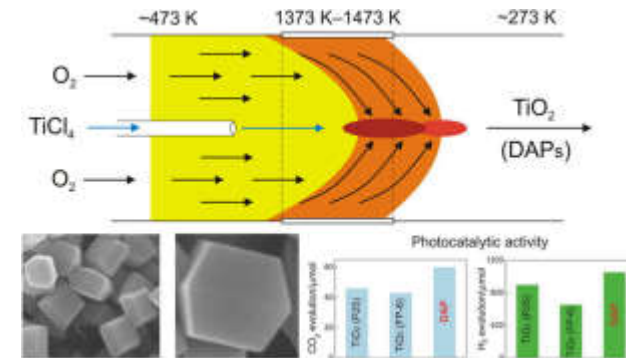
Ashfold et al. 1994. Thin film diamond by chemical vapour deposition methods. *Chemical Society Reviews*, 23, 21-30.

Combustion Synthesis – Traditional Materials

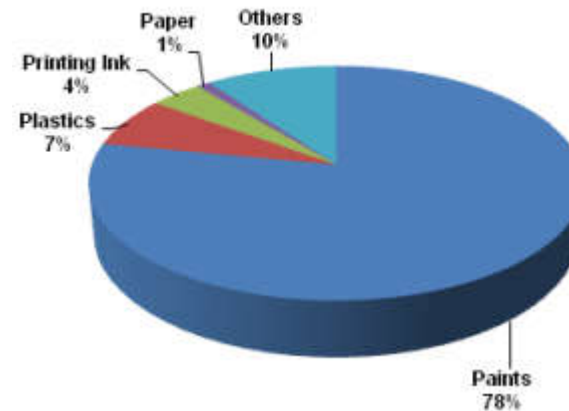
Titania (TiO₂)



Lee, R.F. 1991. *Fifth AusIMM Extractive Metallurgy Conference*. Perth, Australia, 2–4 October 1991. Australasian Institute of Mining and Metallurgy, Parkville, Victoria pp. 35–38.



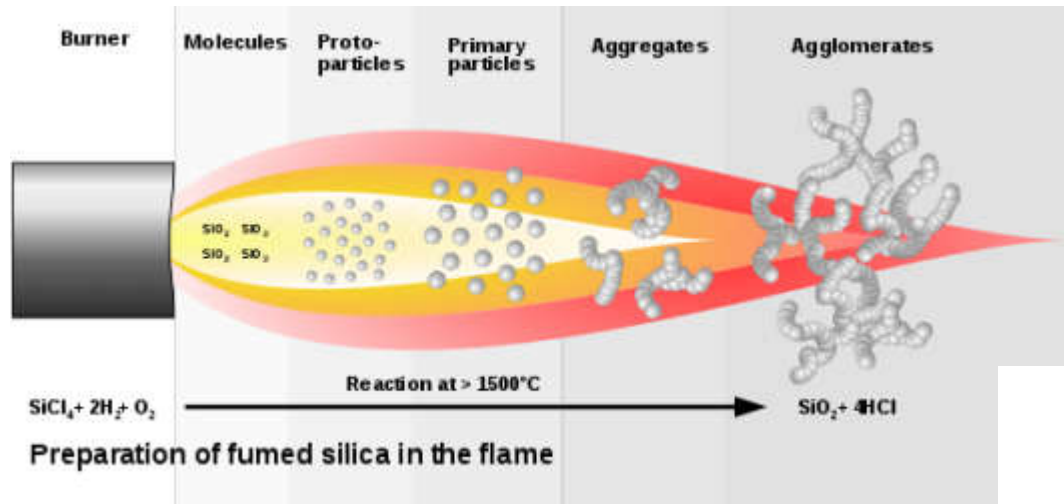
Janczarek et al. (2016) Chem. Eng. J. **289**, pp.502-512.



<http://www.consultmcg.com/blog/titanium-dioxide-tio2-industry-in-india/>

Combustion Synthesis – Traditional Materials

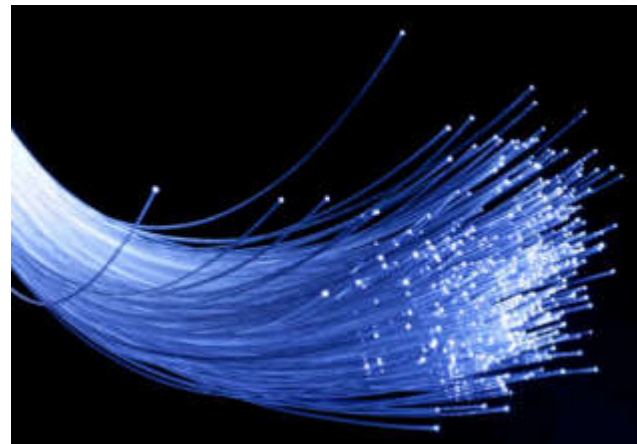
Fumed silica



https://en.wikipedia.org/wiki/Fumed_silica



A raw material for fibre optics



Combustion Synthesis – Traditional Materials

- **Global production (estimates, per year)**
 - Carbon black: 12 million tonnes (\$20 billion)
 - Titania: 7 million tonnes (\$25 billion)
 - Fumed silica: 3 million tonnes (\$2 billion)

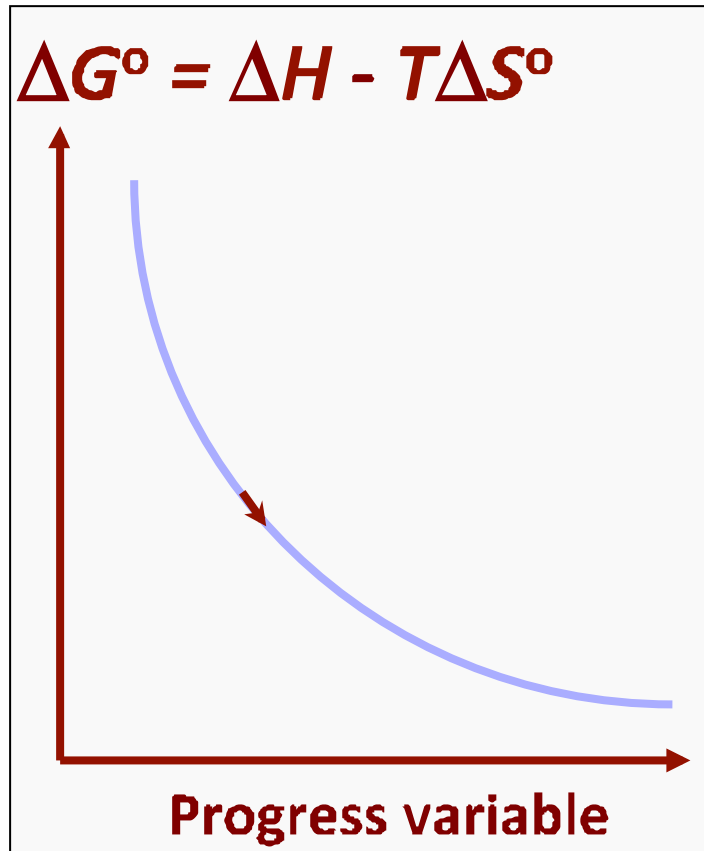
 - Beef: 68 million tonnes

 - SI Engines: \$2 trillion car revenue x ~\$500 engine cost/\$10,000 cost per car = ~\$100 billion/yr
 - Jet engines: \$90 billion/yr

Outline

1. A brief history about earlier applications of nanoparticles
2. Modern applications of nanoparticles: why are they fascinating?
3. Industrial-scale combustion synthesis
- 4. Thermodynamics again**
5. Brief overview of synthesis flames and processes
6. Several case studies
 - “infant” soot as a quantum dot/fluorescent material
 - Titania as an electron transfer media and sensor material
 - Control titania crystal phase using flame stoichiometry

Why Does Condensed-Phase Matter Form in Flames?



Gas-to-Solid Transformation

- **Type 1: enthalpy driven (heat release)**

metal oxides

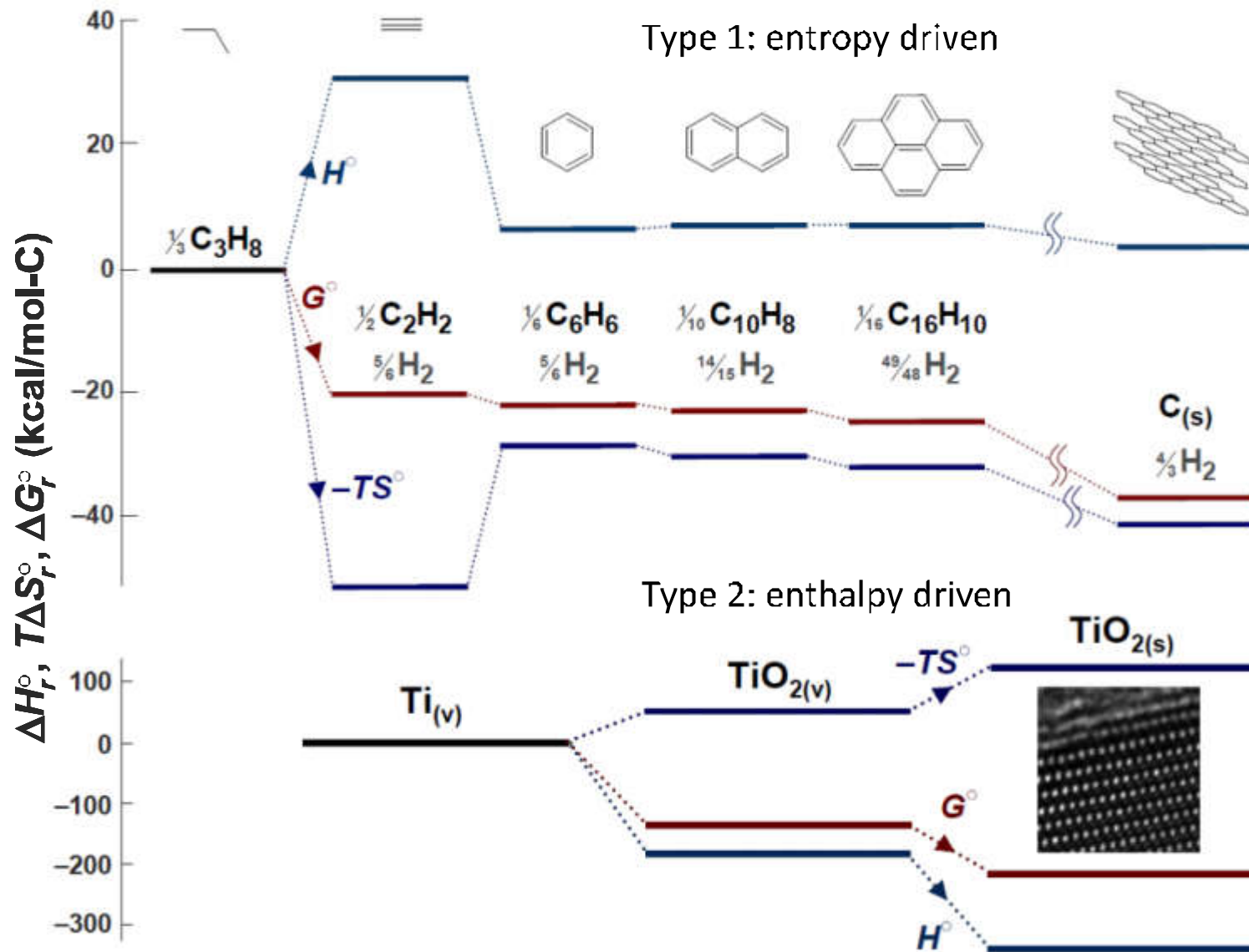
carbides, nitrides etc

- **Type 2: entropy driven**

soot



Free Energy Landscapes

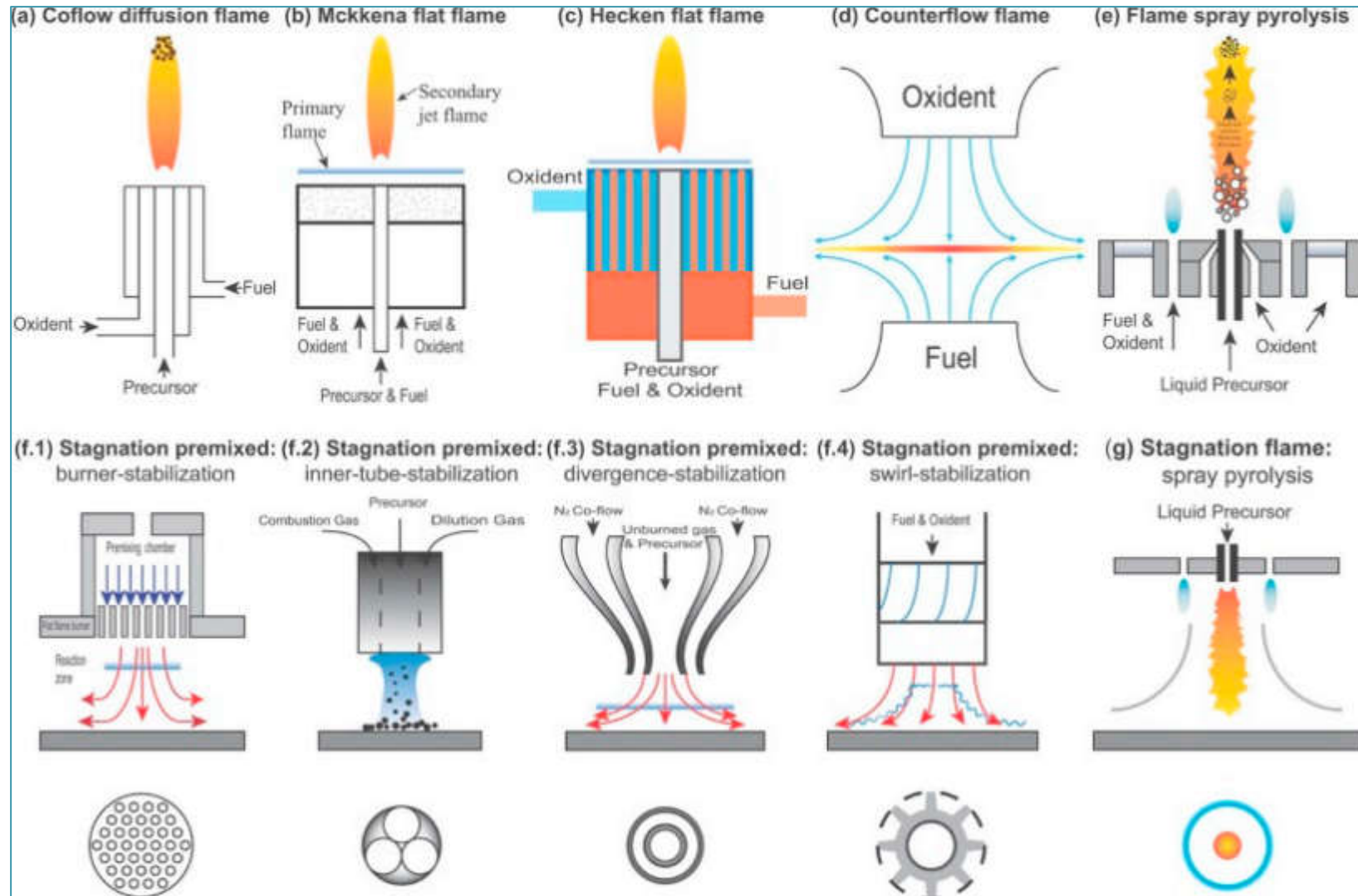


- Control of Type 2 particle formation lies in the control of fluid complexity

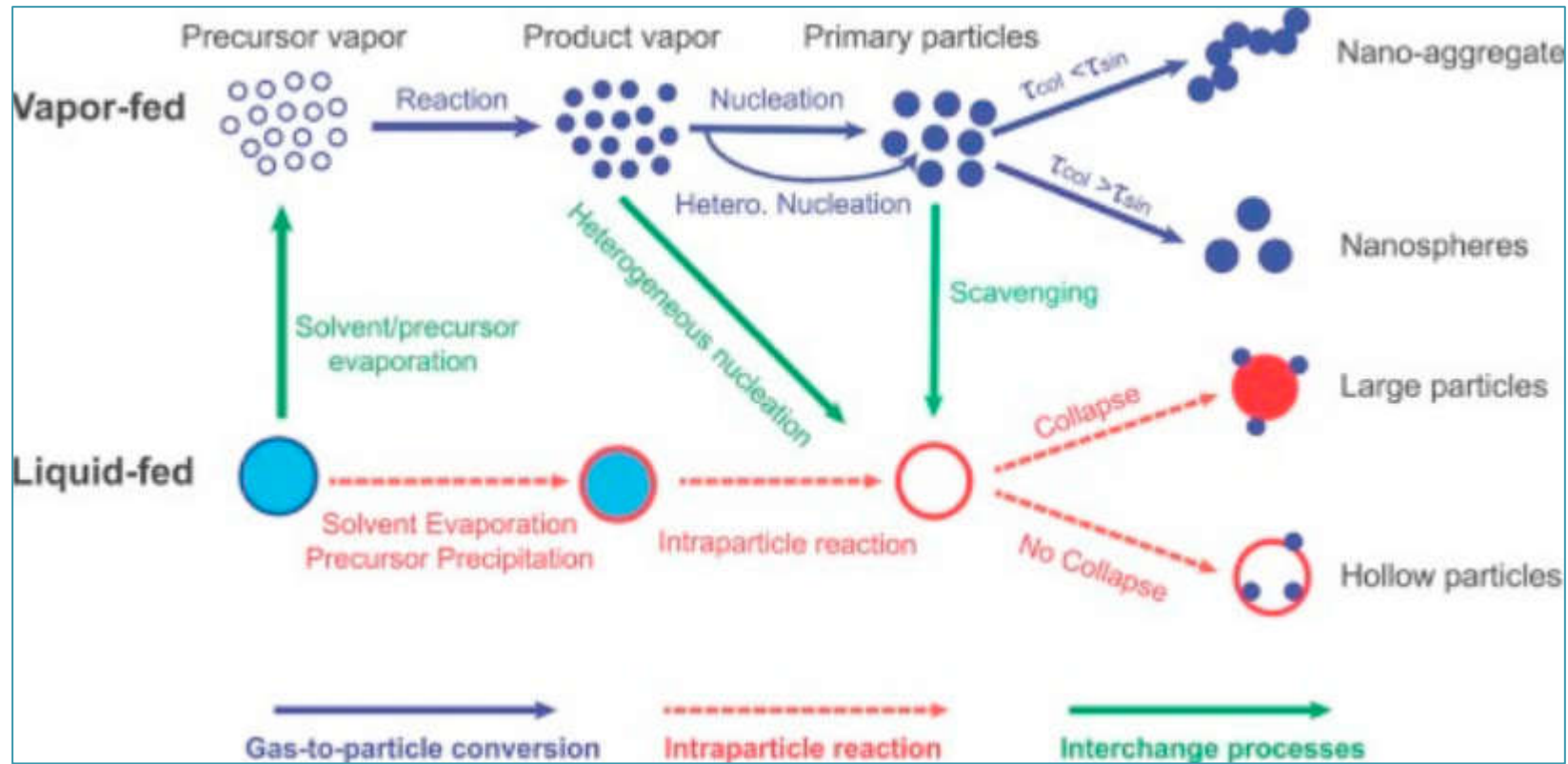
Outline

1. A brief history about earlier applications of nanoparticles
2. Modern applications of nanoparticles: why are they fascinating?
3. Industrial applications of combustion synthesis
4. Thermodynamics again
- 5. Brief overview of synthesis flames and processes**
6. Several case studies
 - “infant” soot as a quantum dot/fluorescent material
 - Titania as an electron transfer media and sensor material
 - Control titania crystal phase using flame stoichiometry

Flame Synthesis Methods



Flame Synthesis Processes



Li et al. 2016 *Prog. Energy Combust. Sci.* **55**, 1-59

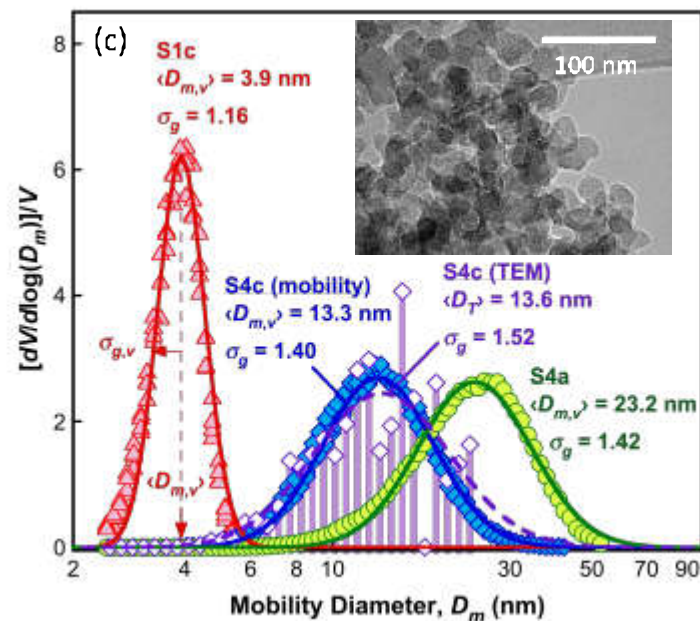
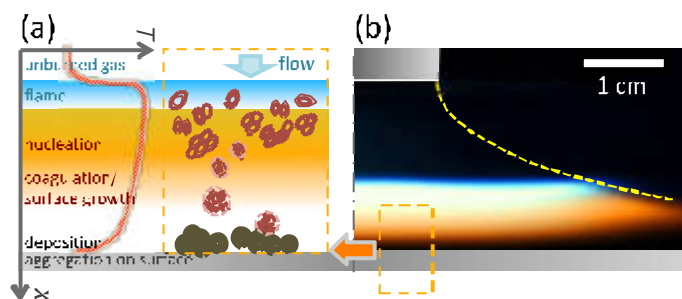
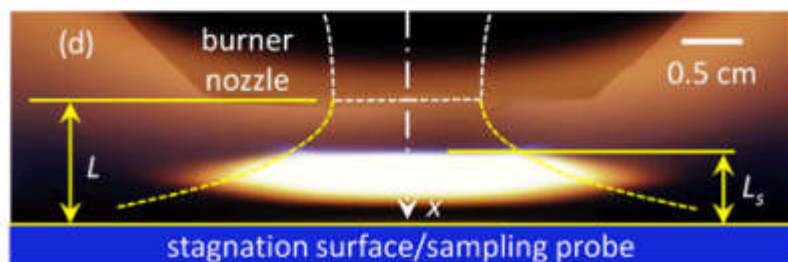
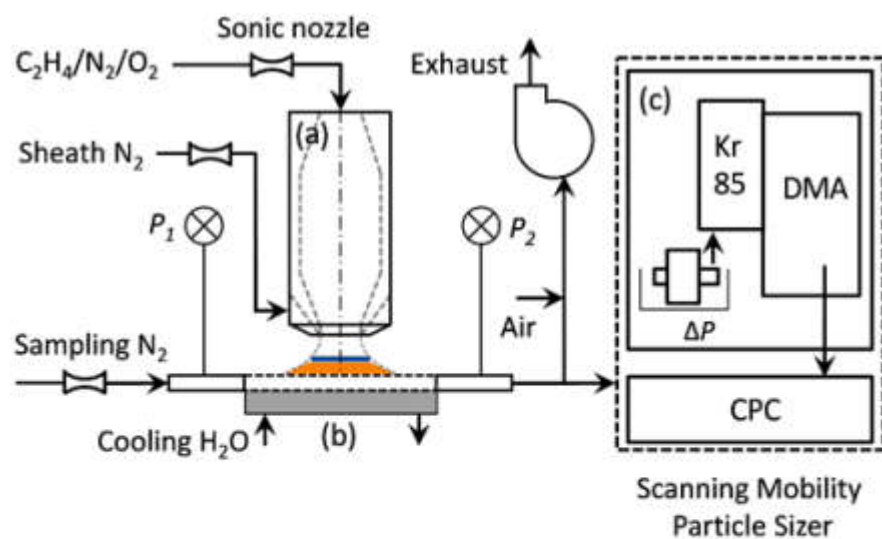
Outline

1. A brief history about earlier applications of nanoparticles
2. Modern applications of nanoparticles: why are they fascinating?
3. Industrial-scale combustion synthesis
4. Thermodynamics again
5. Brief overview of synthesis flames and processes
- 6. Several case studies**
 - “Infant” soot as a quantum dot/fluorescent material
 - Titania as an electron transfer media and sensor material
 - Control titania crystal phase using flame stoichiometry

“Infant” soot as a fascinating material

Example: Fluorescent nanoparticles are promising tools for both optical data storage and applications from biochemical, bioanalytical, to other medical areas

Particle synthesis in premixed stagnation flames



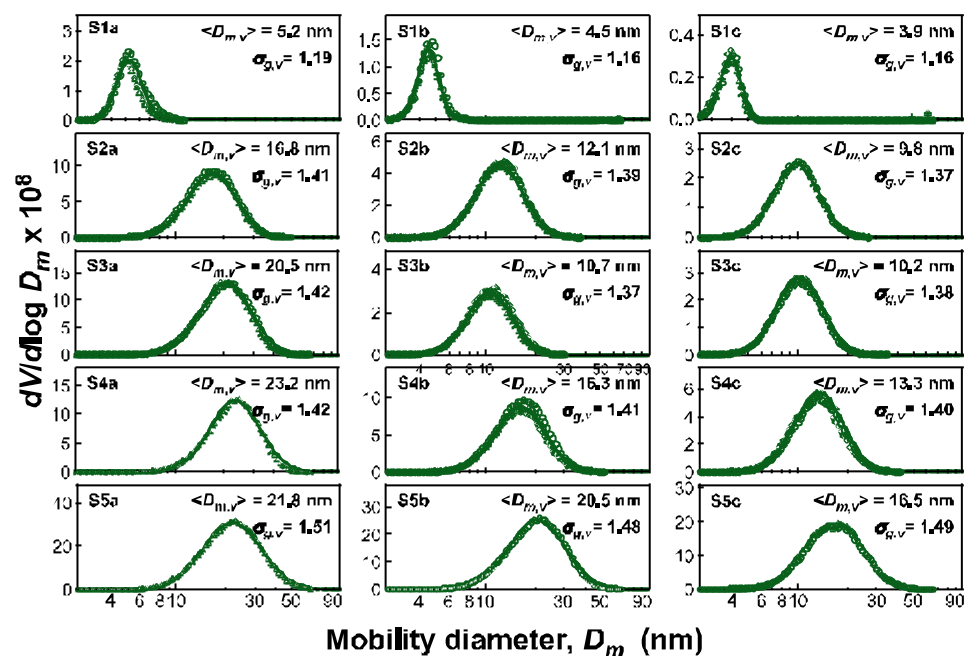
“Infant” soot as a fascinating material

Size variation: 4 to 23 nm

Table S1. Key ethylene stagnation flame parameters^a and median diameter and geometric standard deviation of particles prepared therein.

Flame	V_0^b (cm/s)	$T_n \pm 10$ (K)	$T_s \pm 5$ (K)	L_s^c (mm)	$T_{t,max}^d$ (K)	$\langle D_{m,v} \rangle$ (nm)	$\sigma_{g,v}$
S1: 16.5% C ₂ H ₄ / 20.6% O ₂ / 62.9% N ₂							
a	51	364	345	0.61	2122	5.2	1.19
b	61	382	365	0.54	2132	4.5	1.16
c	74	380	371	0.46	2131	3.9	1.16
S2: 17.3% C ₂ H ₄ / 21.6% O ₂ / 61% N ₂							
a	29	417	350	0.77	2042	16.8	1.41
b	43	428	359	0.57	2052	12.1	1.39
c	51	443	369	0.52	2061	9.8	1.37
S3: 17.4% C ₂ H ₄ / 21.7% O ₂ / 60.9% N ₂							
a	32	440	358	0.80	2010	20.5	1.42
b	44	409	336	0.54	2024	10.7	1.37
c	51	431	354	0.48	2038	10.2	1.38
S4: 17.6% C ₂ H ₄ / 22.0% O ₂ / 60.4% N ₂							
a	35	355	311	0.56	1994	23.2	1.42
b	43	392	338	0.51	2019	16.3	1.41
c	46	424	361	0.52	2036	13.3	1.40
S5: 19.4% C ₂ H ₄ / 24.3% O ₂ / 56.3% N ₂							
a	29	397	324	0.73	1973	21.8	1.51
b	43	388	334	0.59	1969	20.5	1.48
c	51	392	328	0.54	1971	16.5	1.49

^a The equivalence ratio is 2.4. The nozzle-to-stagnation surface separation is 1 cm. ^b V_0 is the “cold” velocity of the unburned gas issued from the nozzle. The values listed are for 298 K and 1 atm, though the actual temperature is higher, as shown in the T_n column. ^c Distance from the stagnation surface to the position of $T_{t,max}$. ^d Modeled using OPPDIF (2) and USC Mech II (3).



“Infant” soot as quantum dots

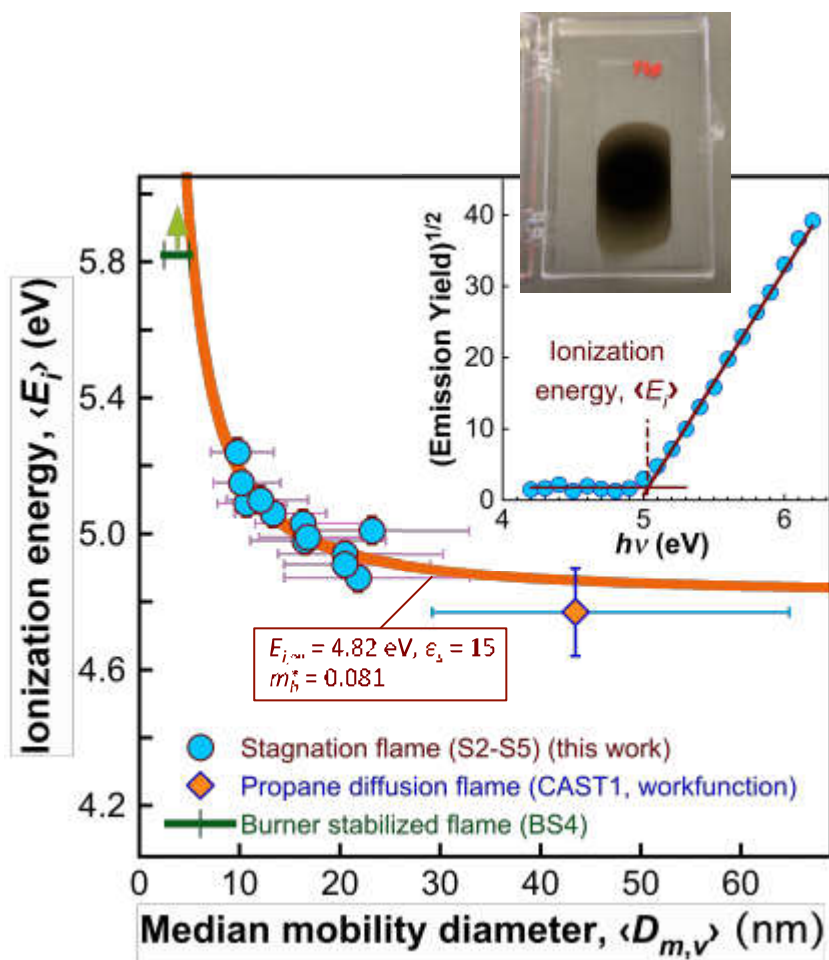
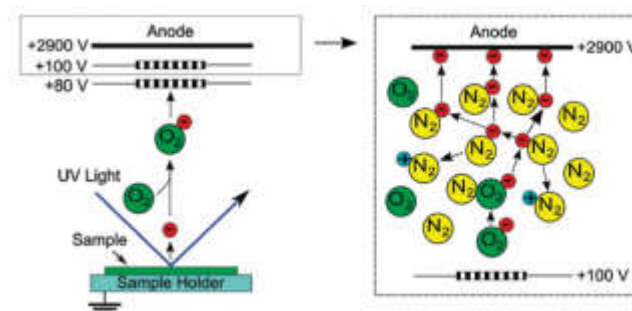


Photo-Emission Spectroscopy in Air (PESA)



Jasieniak et al., *ACS Nano* (2011)

$$\langle E_i \rangle = E_{i,\infty} + \underbrace{\frac{\hbar^2}{2m_h^*} \left\langle \frac{1}{D_{m,v}^2} \right\rangle}_{\text{Quantum confinement}} + \underbrace{\frac{e^2}{4\pi\epsilon_0} \left(\frac{1}{\epsilon_{air}} - \frac{1}{\epsilon_s} \right) \left\langle \frac{1}{D_{m,v}} \right\rangle}_{\text{Image charge potential}}$$

Table 1. Parameters of Eqs. (1) and (3).

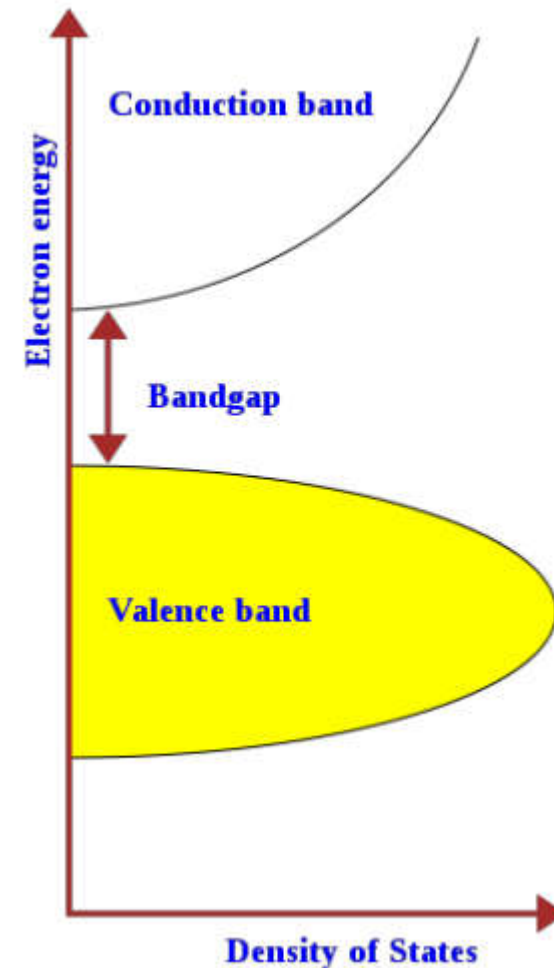
$E_{i,\infty} = 4.82$ eV	$E_{g,i,\infty}^{sp} = 0.12$ eV	$\epsilon_s = 15$	$m_h^* = 0.081$	$m_v^* = 0.176$
--------------------------	---------------------------------	-------------------	-----------------	-----------------

Band Gap

- The minimum energy gap between the valence and conduction bands, which can either be direct or indirect depending on the type of transitions
- The optical bandgap is commonly determined from the UV-Visible absorption spectrum using the Tauc model¹⁻²

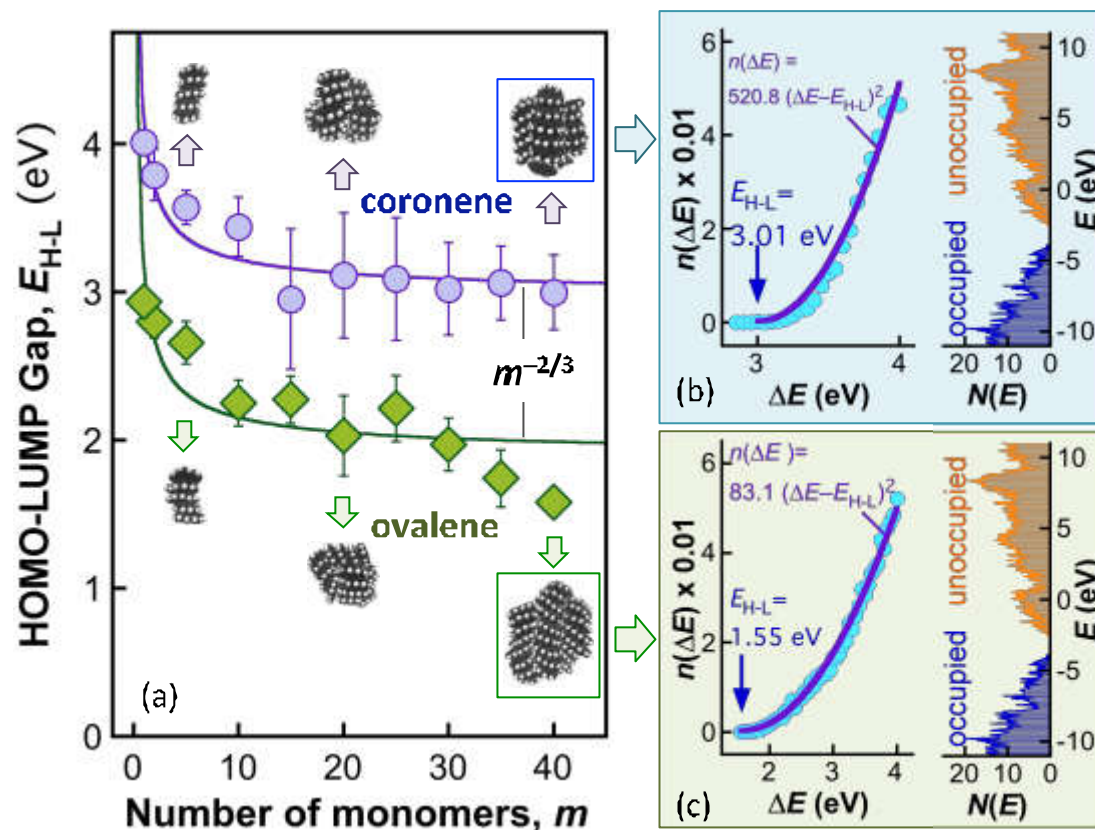
$$(\alpha h\nu)^{1/n} = B(h\nu - E_g^{opt})$$

- Depending on the type of transitions, the power index “ n ” takes on different values for direct and indirect bandgap materials
- Mott and Davis suggest $n = 2$ for indirect bandgap and $n = 1/2$ for direct bandgap material²



[1] Tauc, J., Materials Research Bulletin, 3 (1968) 37-46.
[2] Davis, E. A., Mott, N., Philosophical Magazine, 22 (1970) 903-922.

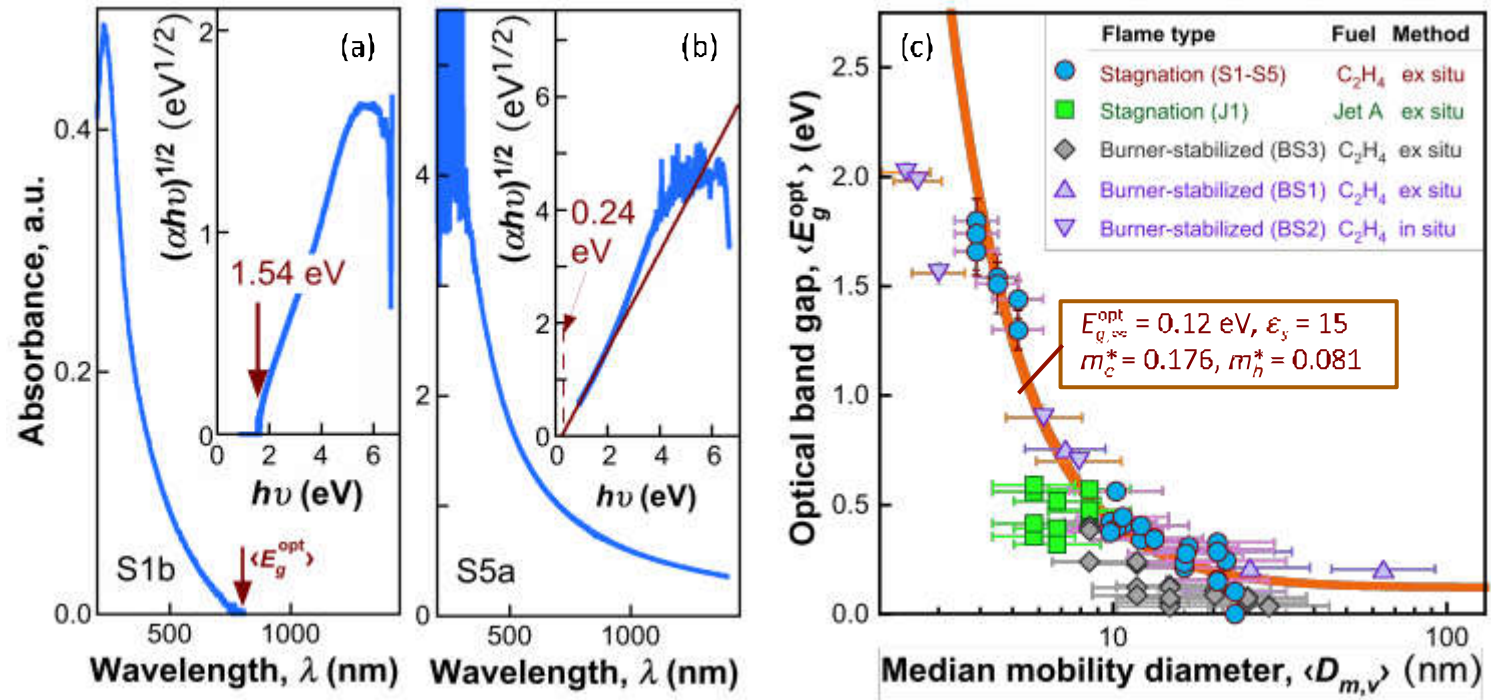
“Infant” soot as quantum dots



(a) B3LYP/6-31G(d) HOMO-LUMO energy gap E_{H-L} for coronene and ovalene clusters.

(b) and (c): Densities of occupied and unoccupied energy states and density of allowable transitions for the coronene₄₀ and ovalene₄₀ clusters, respectively. The lines are fits to the calculated $n(\Delta E)$ using an exponent value of $n = 2$ (an indirect semiconductor)

“Infant” soot as quantum dots



Brus Theory

$$\langle E_g^{\text{opt}} \rangle = E_{g,\infty}^{\text{opt}} + \underbrace{\frac{\hbar^2}{2} \left(\frac{1}{m_c^*} + \frac{1}{m_h^*} \right)}_{\text{Quantum confinement}} \left\langle \frac{1}{D_{m,v}} \right\rangle - \underbrace{\frac{1.8e^2}{2\pi\epsilon_0\epsilon_s}}_{\text{Coulomb electron-hole interaction}} \left\langle \frac{1}{D_{m,v}} \right\rangle$$

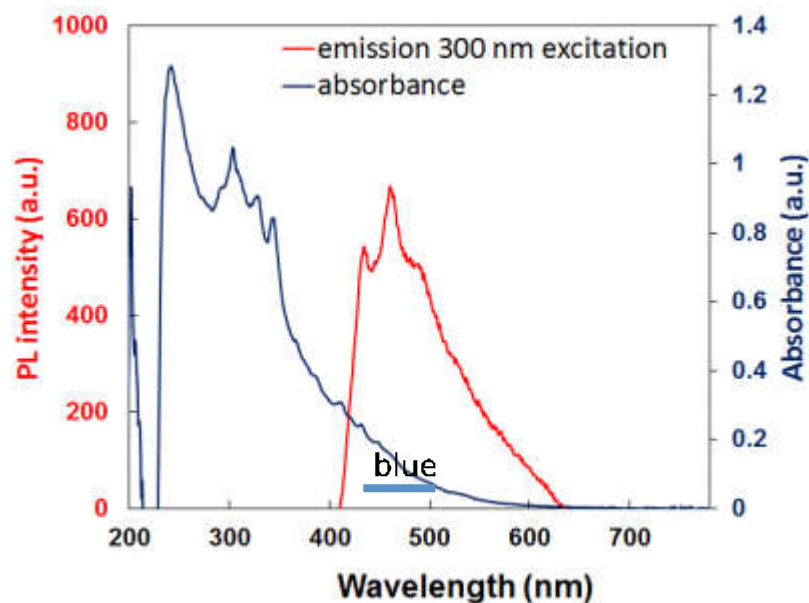
Quantum
confinement

Coulomb electron-
hole interaction

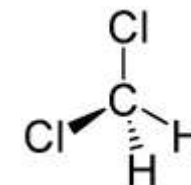
Table 1. Parameters of Eqs. (1) and (3).

$$E_{g,\infty}^{\text{opt}} = 4.82 \text{ eV} \quad E_{g,\infty}^{\text{opt}} = 0.12 \text{ eV} \quad \epsilon_s = 15 \quad m_h^* = 0.081 \quad m_c^* = 0.176$$

“Infant” soot as quantum dots

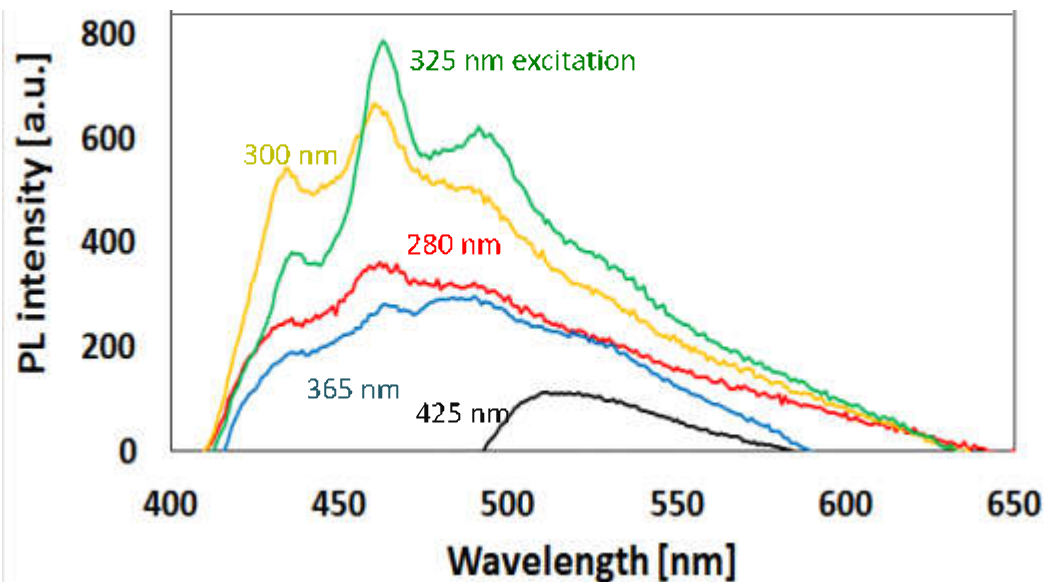


Dichloromethane
(low polarity
solvent)

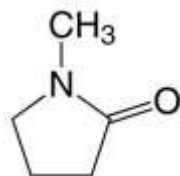


DCM
only

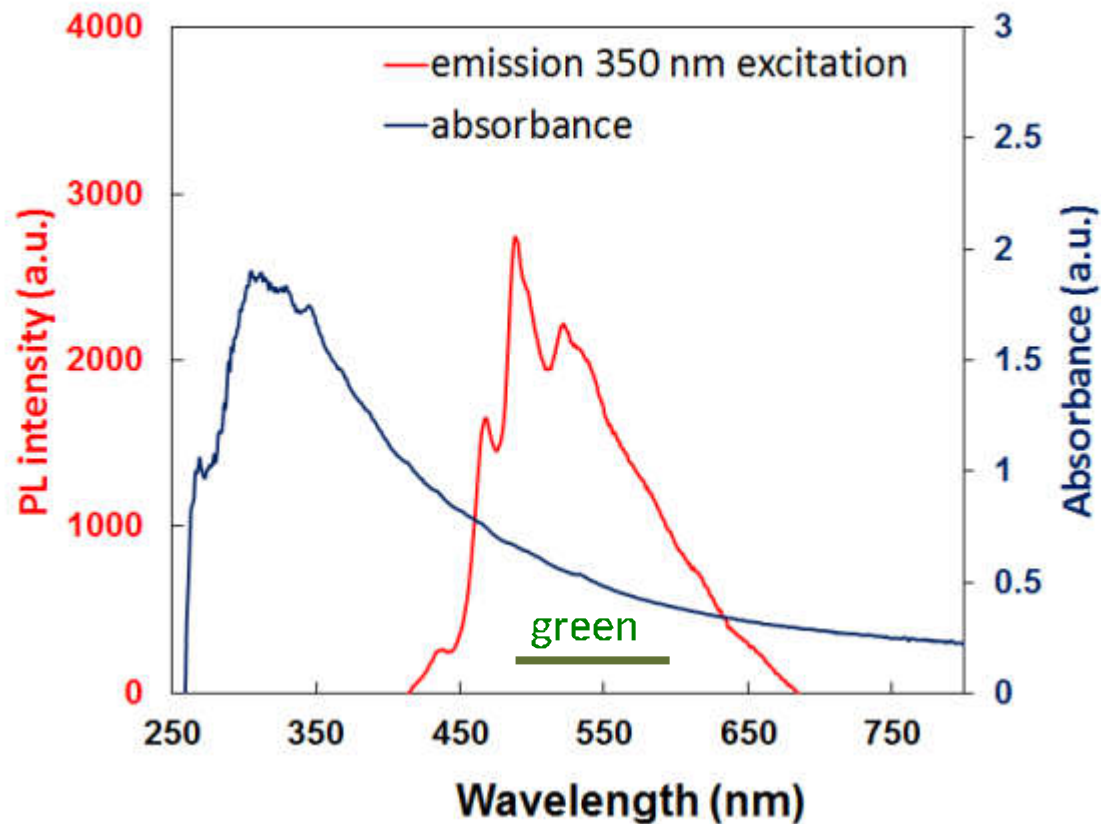
DCM +
"infant" soot



“Infant” soot as quantum dots



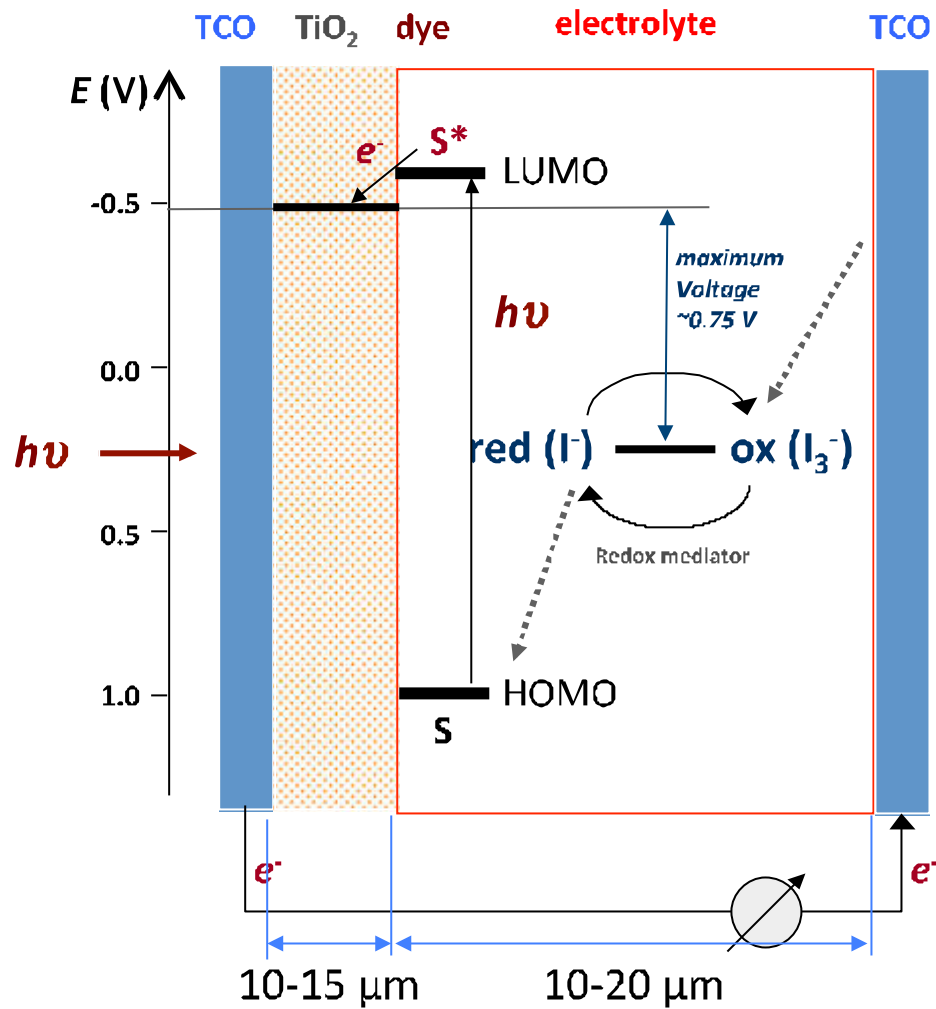
N-methylpyrrolidone
(high polarity solvent)



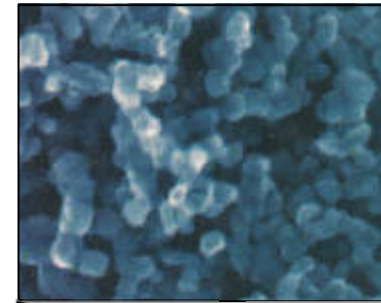
Outline

1. A brief history about earlier applications of nanoparticles
2. Modern applications of nanoparticles: why are they fascinating?
3. Industrial-scale combustion synthesis
4. Thermodynamics again
5. Brief overview of synthesis flames and processes
- 6. Several case studies**
 - “Infant” soot as a quantum dot/fluorescent material
 - **Titania as an electron transfer media and sensor material**
 - Control titania crystal phase using flame stoichiometry

Dye-Sensitized Solar Cell (DSSC)

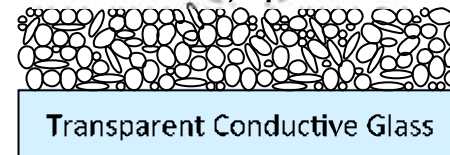


Mesoporous Layer

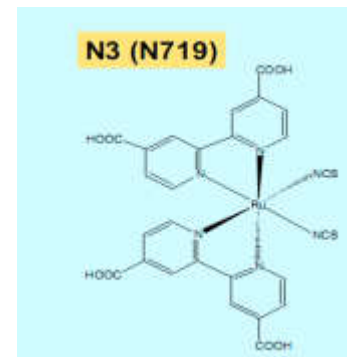


Film of anatase TiO_2
 ~ 20 nm in diameter

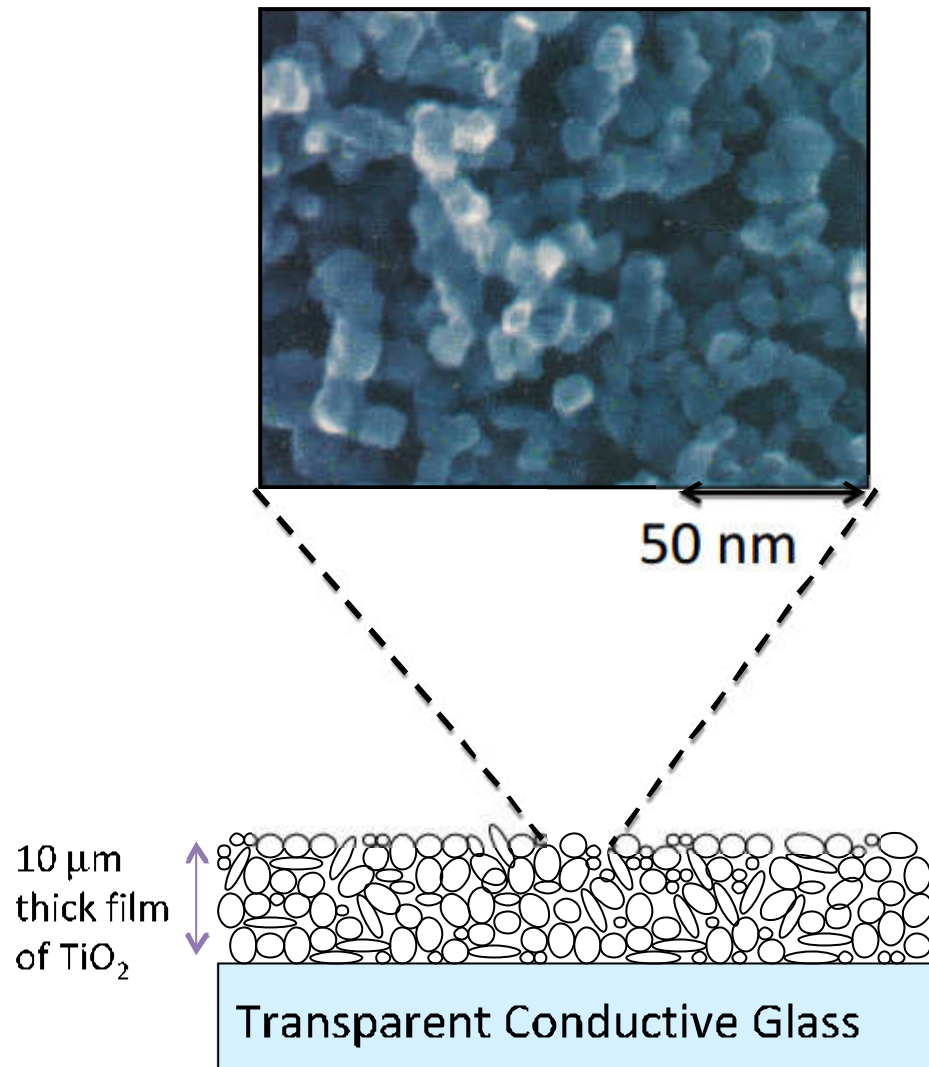
Usually produced by Sol
 Gel



Sensitizing Dye



Anode Characteristics



- **Single crystal TiO₂** particles
- Phase pure **anatase**
- Thickness of $\sim 10 \mu\text{m}$
- Large surface area for dye adsorption
- High electron diffusivity

Synthesis Routes

- Laser ablation
- Spray pyrolysis
- Chemical vapor deposition
- Flame
- **Sol/Gel**

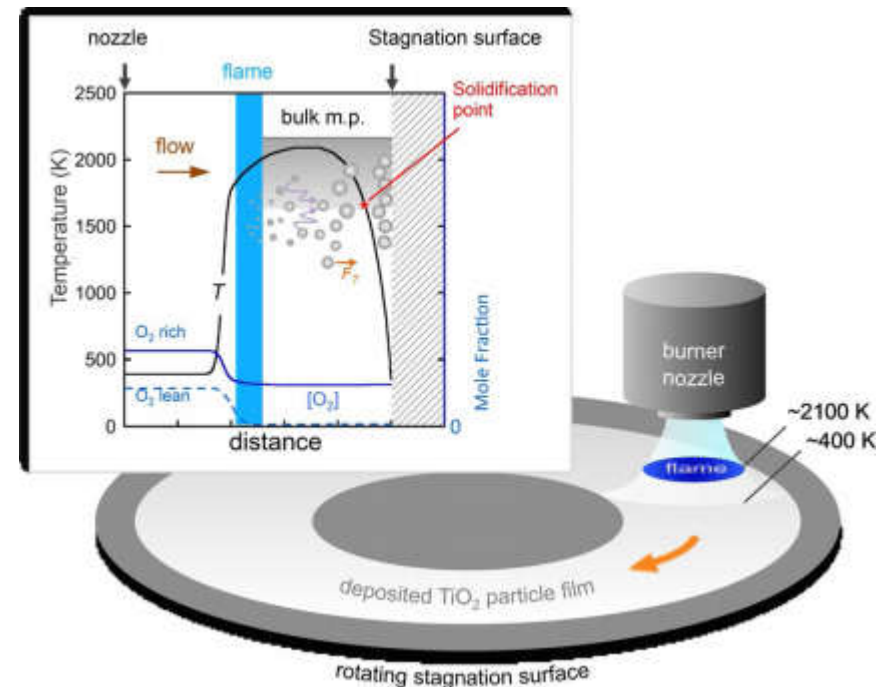
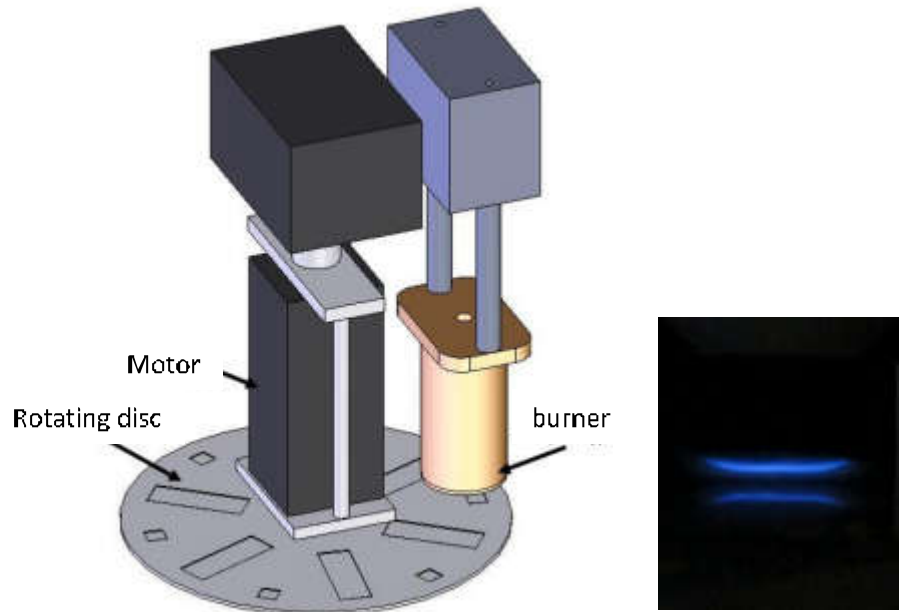
The Problem

“For the best performing TiO_2 electrodes, the synthesis of TiO_2 paste involves hydrolysis of $\text{Ti}(\text{OCH}(\text{CH}_3)_2)_4$ in water to ethanol by three times centrifugation. Finally, the ethanol is exchanged with α -terpineol by sonication and evaporation. **Totally, it takes 3 days. Such a long time procedure of TiO_2 paste is economically unsuitable for industrial production and has to be reduced.**”

Michael Gratzel *Prog. Photovolt.* 2007; 15:603-612

Flame Stabilized on Rotating Surface (FSRS)

A method of one-step particle synthesis/film processing

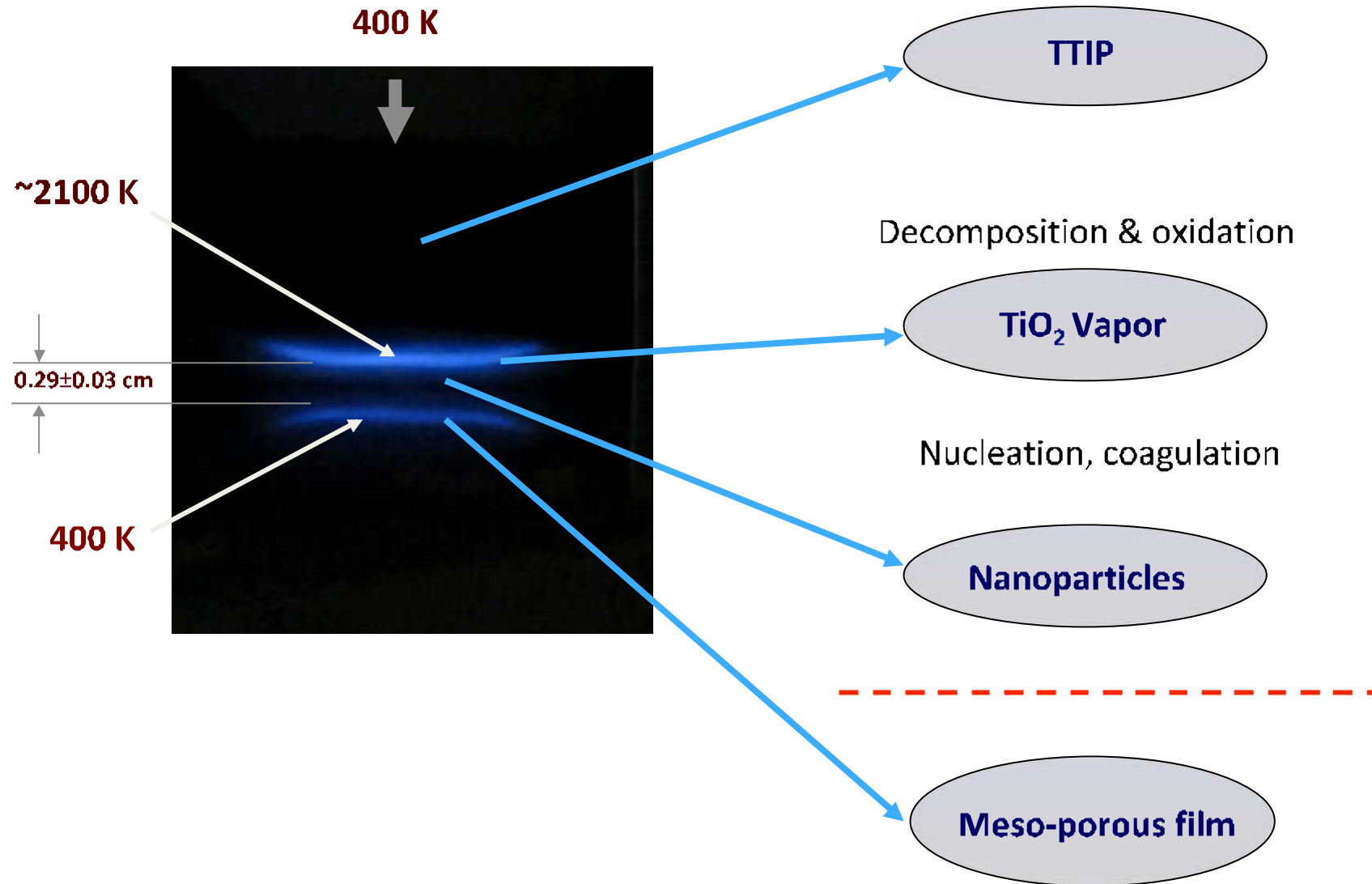


- Aerodynamically shaped nozzle
($D = 1$ cm)
- Nozzle-to-disc distance
($L = 3.0$ cm)
- 30.5 cm rotating disc (0 to 600 RPM)

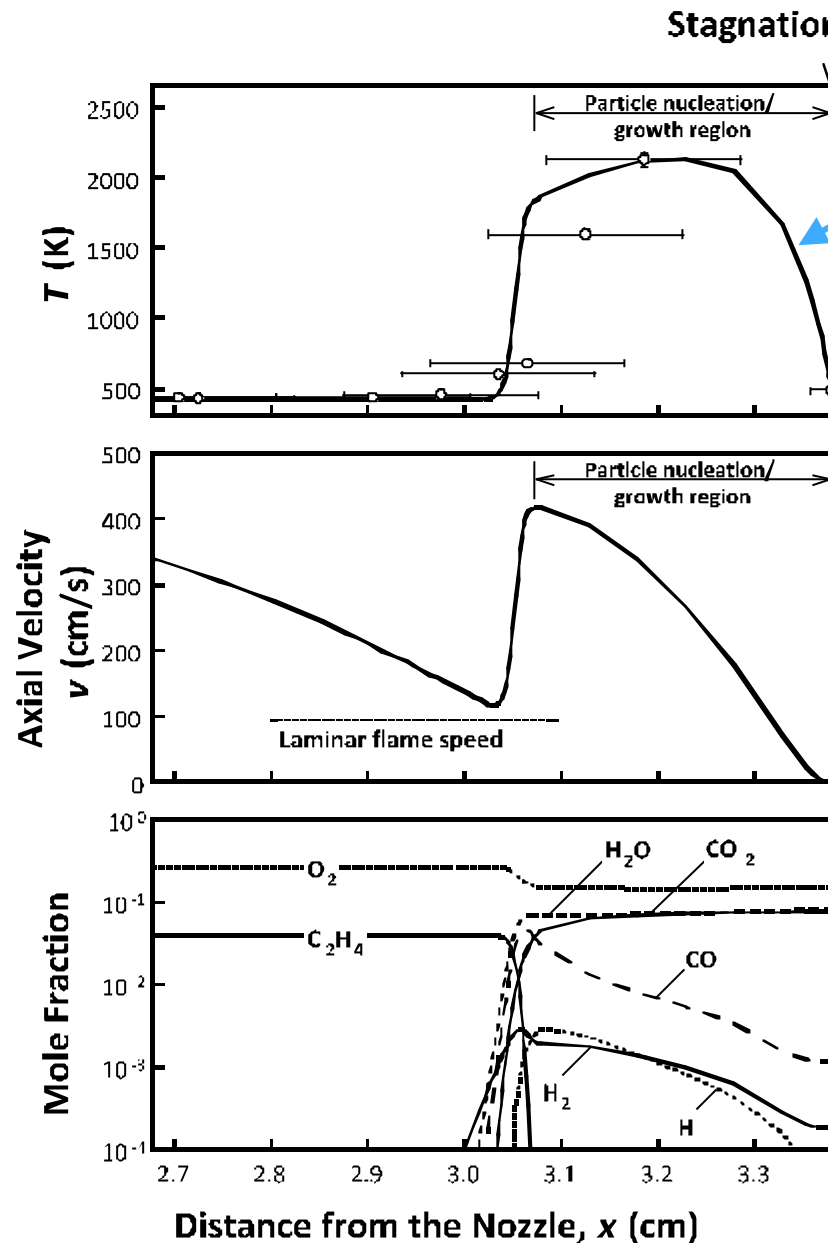
- Flame diameter ~ 3 cm
- Flame-to-disc distance 0.29 ± 0.03 cm

Tolmochoff et al. *PROCI* 2009
Memarzadeh et al. *PROCI* 2011
Nikratz et al. *JPC* 2012 46

Mechanism of Particle Formation and Deposition

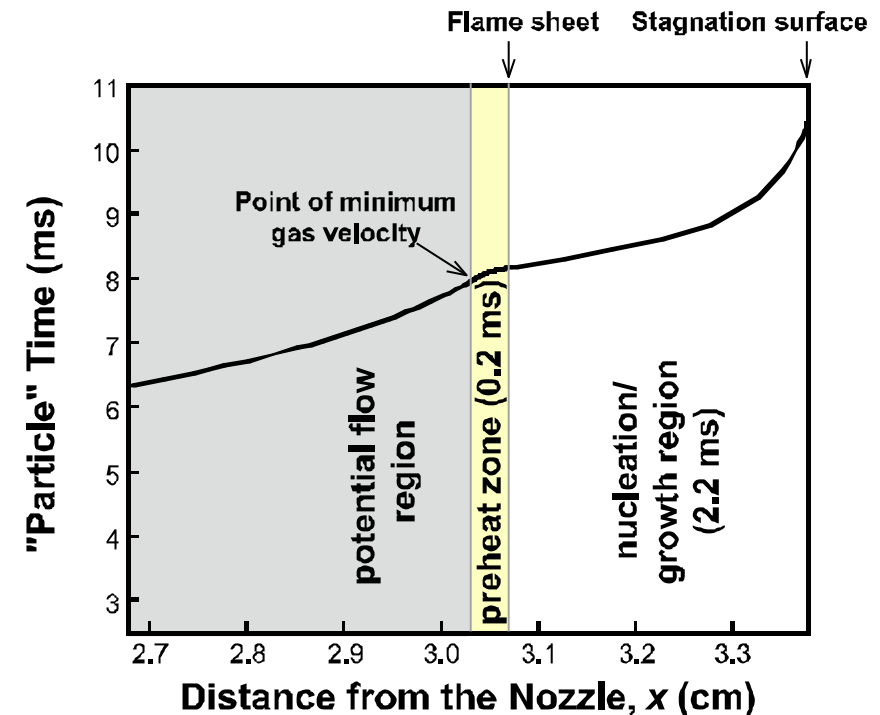


Flame Structure (Ethylene-oxygen-argon, $\phi = 0.4$)



Thermophoretic velocity by Waldmann theory

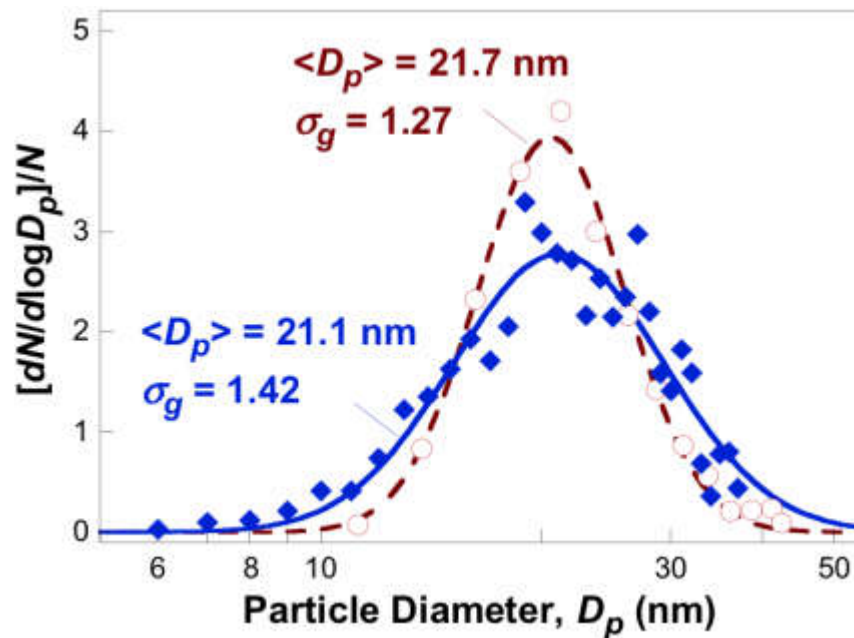
$$v_{T,1} = \frac{\kappa}{Nk_e} \frac{dnT}{dx}$$



Computations used the Sandia counterflow flame code and USC Mech II

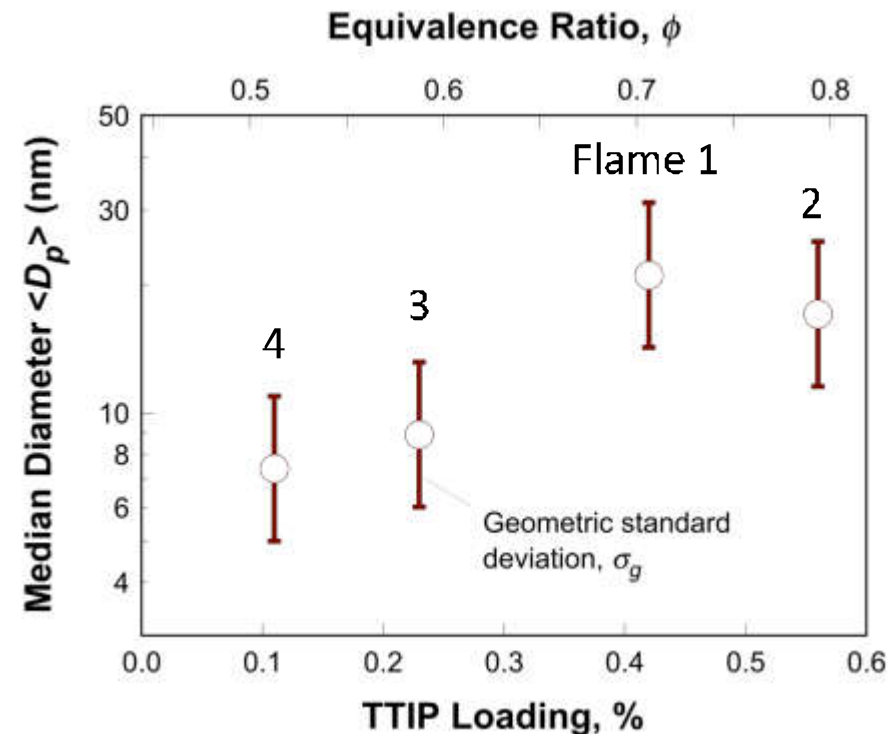
Particle Properties: Diameter

Matching the size distribution of the champion cell using Flame 1

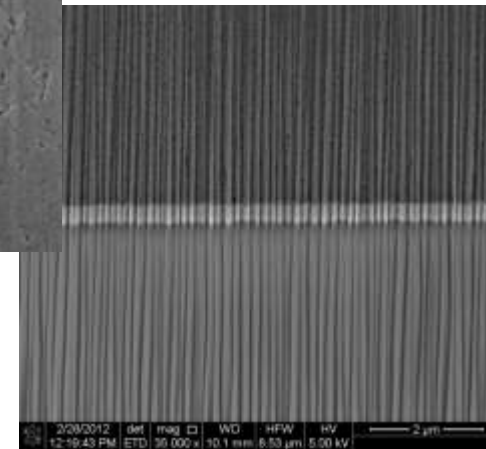
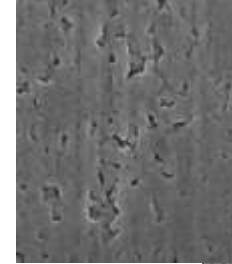
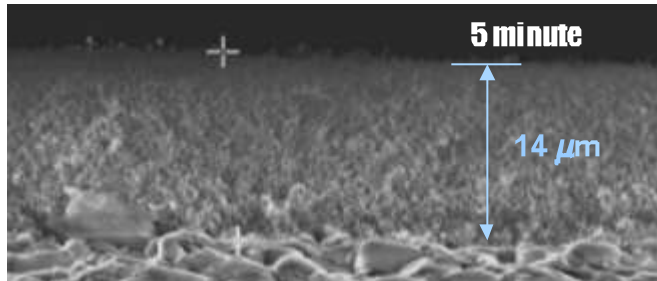
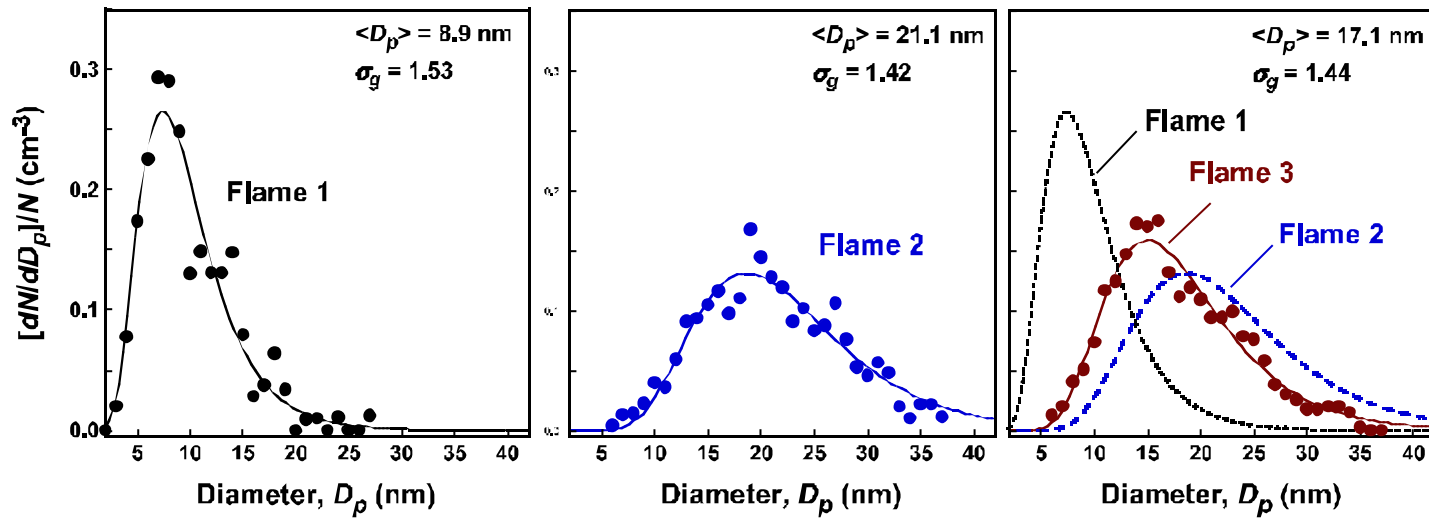


Source: M. Gratzel, *Journal of Photochemistry and Photobiology C-Photochemistry Reviews* 2003, 4, (2), 145-153

Size variation achieved through changes in Ti precursor loading



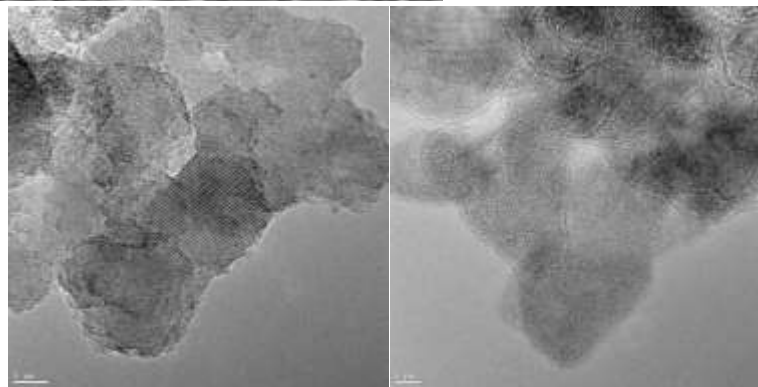
Particle Size Distributions and Film Properties



TiO_2

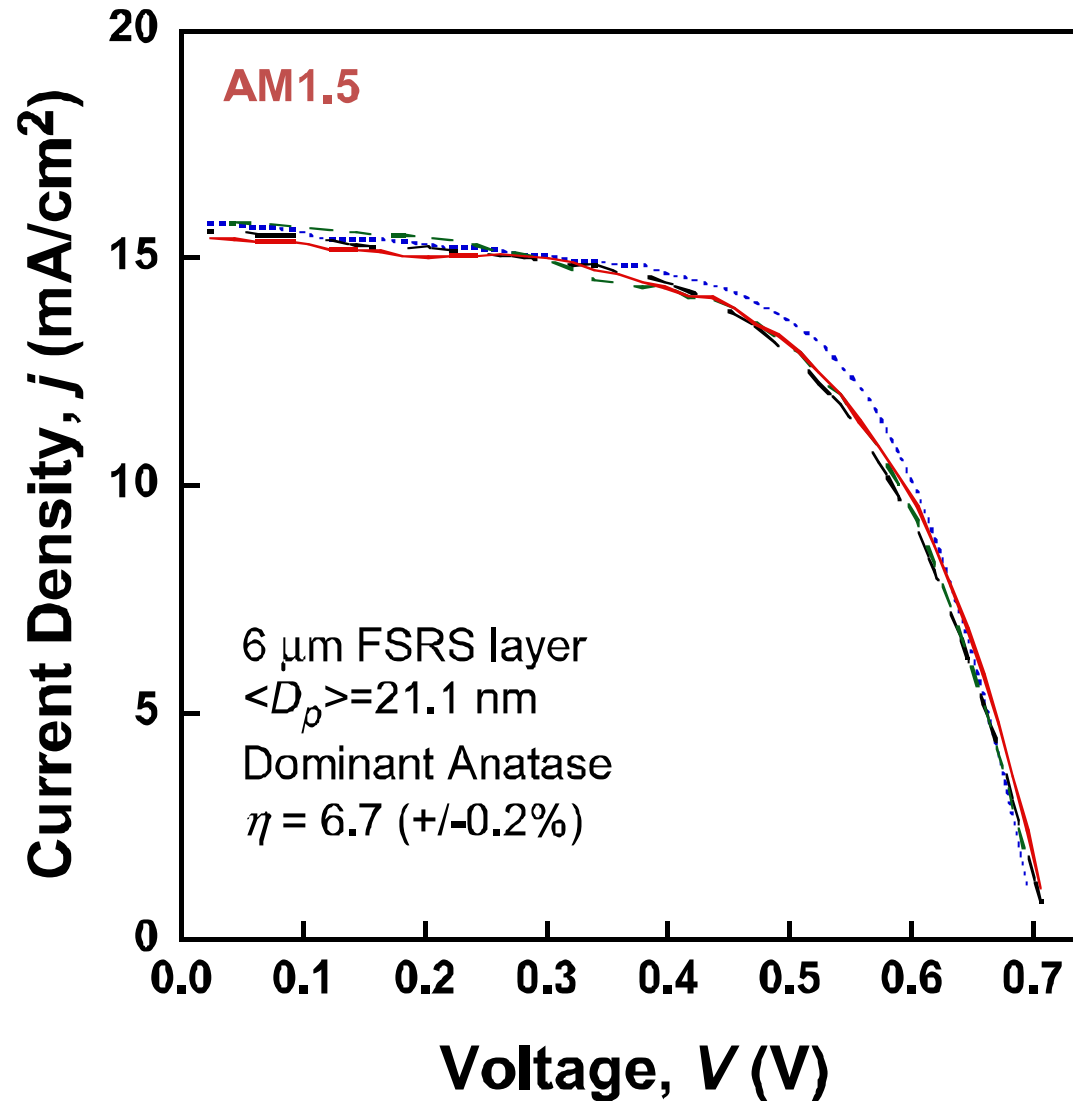
TCO

Glass

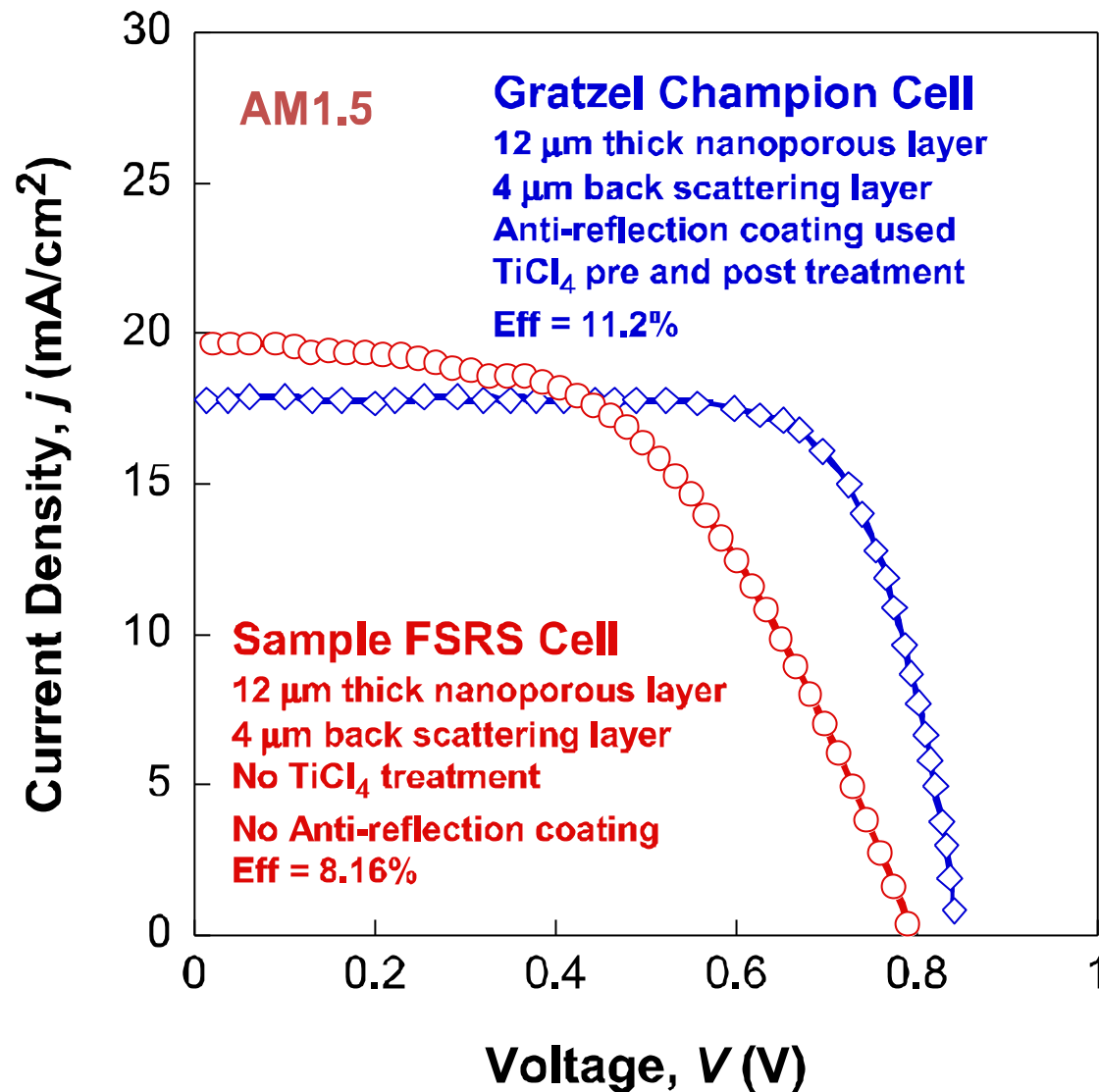


Well-sintered, crystalline anatase particles

DSSC I-V Curves are Reproducible



Can FSRS achieve Sol-Gel efficiency?



Titania Film Chemical Sensors

- The same film on an inter-digitated chip operates as an ultra-sensitive CO sensor.
- The electric conductance of semi-conductor metal oxide becomes ultra sensitive to surface composition when the size < Debye length.
- Gas-surface reaction equilibrium determines the surface oxygen concentration, which in turn, impacts the electric conductivity
- CO detection sensitivity reaches PPM levels

Surface reaction mechanism:

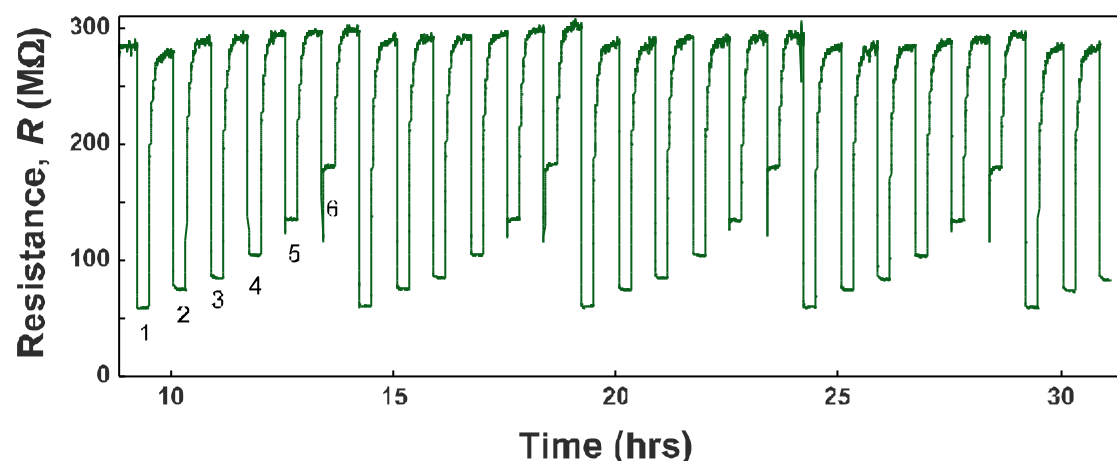
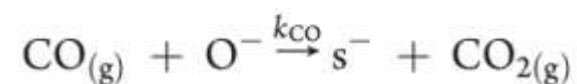
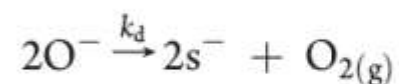
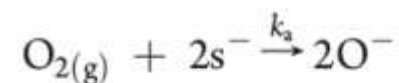


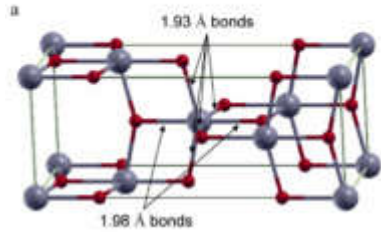
Figure 5. Responses of directly deposited FSRS sensor (sample FSRS-2) to CO exposure at 773 K. Labels 1 through 6 correspond to 280, 140, 93, 46, 18, and 5 PPM CO in air, respectively. The signal overshoot at 18 and 5 PPM CO is due to overshoot of the mass flow controller.

Outline

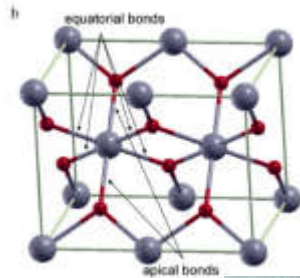
1. A brief history about earlier applications of nanoparticles
2. Modern applications of nanoparticles: why are they fascinating?
3. Industrial-scale combustion synthesis
4. Thermodynamics again
5. Brief overview of synthesis flames and processes
- 6. Several case studies**
 - “Infant” soot as a quantum dot/fluorescent material
 - Titania as an electron transfer media and sensor material
 - **Control titania crystal phase using flame stoichiometry**

Two Most Dominant Crystal Phases of TiO₂

Anatase: metastable in bulk



Rutile



Polymorphs	Rutile		Anatase	
	c	⊥c	c	⊥c
Crystal structure	Tetragonal		Tetragonal	
	$c = 2.9587\text{Å}$ [470]	$a = 4.5937\text{Å}$ [470]	$c = 9.5146\text{Å}$ [93]	$a = 3.7842\text{Å}$ [93]
Space group	$P4_2/mnm$ (136) [84]		$I4_1/amd$ (141) [84]	
Most stable state	(110) [94]		(101) [102]	
Density	4.25 g/cc [84]		3.89 g/cc [84]	
Band gap at 10 K	3.051 eV [471,472]	3.035 eV [471,472]	3.46 eV [35]	3.42 eV [35]
Spectral dependence	$E^{1/2}$ [35]	$E^{1/2}$ [35]	Urbach [40]	
Nature of gap	Indirect [471,472]	Direct [471,472]	Indirect [35]	Direct [35]
Static dielectric constant (ϵ_s , in MHz range)	173 [13,473]	89 [13,473]	48 [474]	31 [475]
High frequency dielectric constant, ϵ_∞ ($\lambda = 600$ nm)	8.35 [103]	6.76 [103]	6.25 [41]	6.50 [41]
Refractive index (at $\lambda = 600$ nm)	2.89 [103]	2.60 [103]	2.50 [41]	2.55 [41]
Nature of conductivity at room temperature (undoped)	n-Type semiconductor [21,112]			
Mott transition	Not observed [118]		Observed [35]	
Room temperature mobility in crystal	0.1–1 cm ² /vs [22,81]		15 cm ² /vs [35,112]	
	0.01 cm ² /vs (high impurity concentration) [81]			
	$\mu_{\text{ps}} = (2-5) * \mu_{\text{is}}$ [22,476]			
Room temperature mobility in polycrystalline thin film	0.6–1.5 cm ² /vs [476]	0.6–1.5 cm ² /vs [476]	0.1–4 cm ² /vs [35]	
	0.1 cm ² /vs [22,38] CUA			

Bulk versus Surface Free Energy

TiO₂
nanoparticles
w/o surface
oxygen vacancy

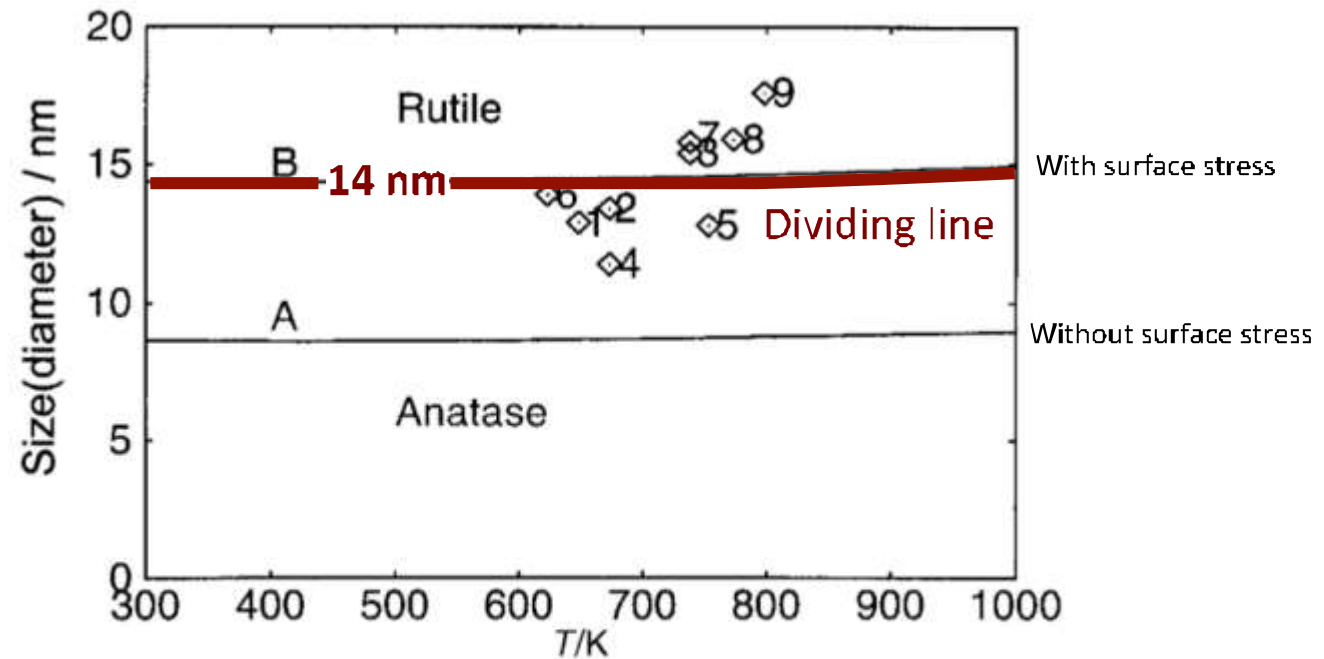
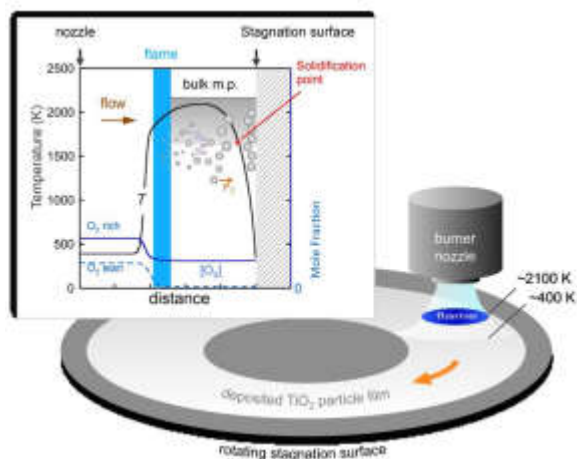


Fig. 2 Phase boundary between nanocrystalline anatase and rutile. Line A: calculated without consideration of surface stress [eqn. (4)]; line B: calculated with consideration of surface stress [eqn. (7), assuming surface stress takes the value of surface free energy, or $t = 1$]. Points: experimental data from ref. 1 (see Table 1).

$$\Delta G^0 = \Delta_f G^0(T, \text{rutile}) - \Delta_f G^0(T, \text{anatase}) + (2t + 3) \frac{M}{r} \left(\frac{\gamma_R}{\rho_R} - \frac{\gamma_A}{\rho_A} \right)$$

Bulk: $\Delta_f G^0(T, \text{rutile}) < \Delta_f G^0(T, \text{anatase})$ Surface: $\gamma_R > \gamma_A$

Contradicting Evidence from Flame Synthesis



X-ray diffraction shows that flame synthesized TiO_2 nanoparticles can be both rutile and anatase

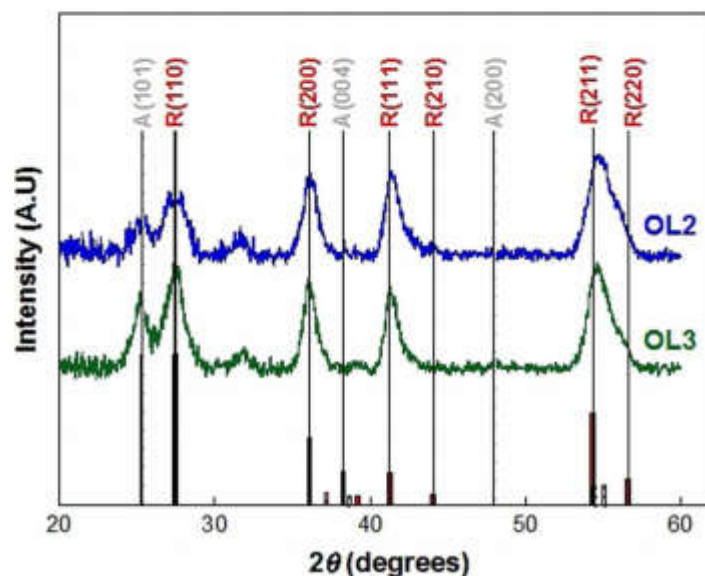
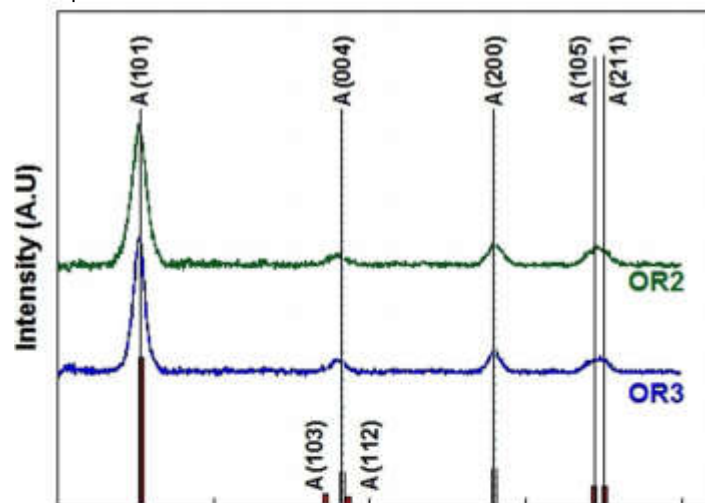
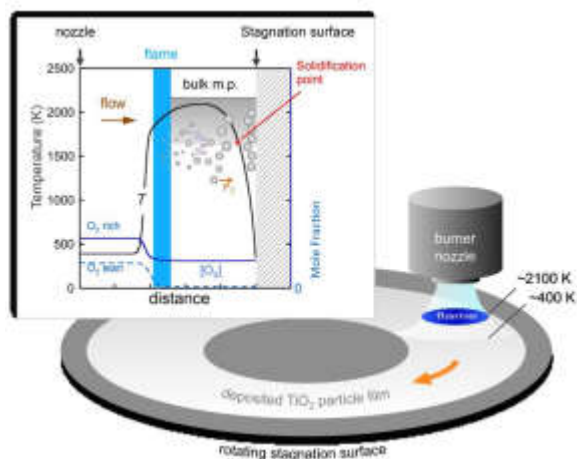


Table 1. Flame equivalence ratio (ϕ), adiabatic temperature (T_{ad}), equilibrium O_2 mole fraction ($x_{\text{O}_2,eq}$), crystallite size and phase data of the TiO_2 particles synthesized.

Flame	ϕ	T_{ad} [K]	$x_{\text{O}_2,eq}$	Crystallite size [nm] ^[a]	%(wt) anatase ^[b]
OR1	0.44	2385	1.8×10^{-1}	< 5	78
OR2	0.46	2329	1.5×10^{-1}	11.3	93
OR3	0.59	2667	1.5×10^{-1}	17.7	94
OL1	1.19	2557	3.3×10^{-3}	< 5	30
OL2	1.15	2560	4.4×10^{-3}	7.5	26
OL3	1.33	2606	1.7×10^{-3}	12.1	29
1a ^c	0.52	2354	1.3×10^{-1}	11	91
1b ^c	0.68	2551	8.5×10^{-2}	13	95
1c ^c	0.83	2652	5.4×10^{-2}	13	71
2a ^c	0.90	2651	3.7×10^{-2}	11	98
3a ^c	1.13	2782	1.6×10^{-2}	8	20
4a ^c	1.27	2797	9.3×10^{-3}	9	12

[a] as determined by XRD. [b] the balance is rutile. [c] taken from Memarzadeh et al.^[27]

Contradicting Evidence from Flame Synthesis

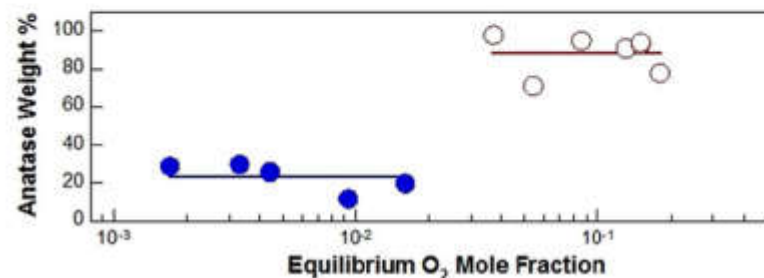
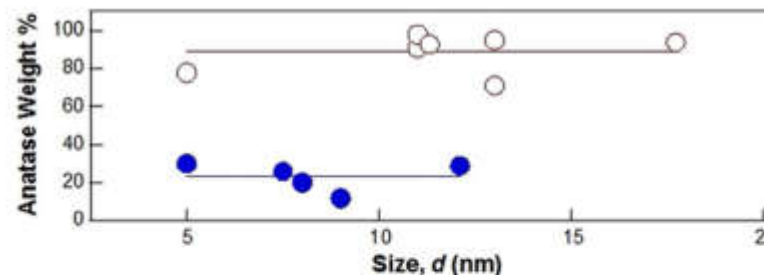


X-ray diffraction also shows that the crystal phase of flame-synthesized TiO_2 is independent of the size, but it depends on the flame stoichiometry.

Table 1. Flame equivalence ratio (ϕ), adiabatic temperature (T_{ad}), equilibrium O_2 mole fraction ($x_{\text{O}_2,eq}$), crystallite size and phase data of the TiO_2 particles synthesized.

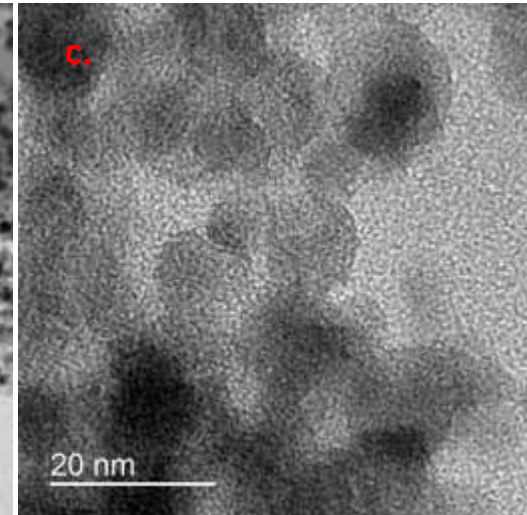
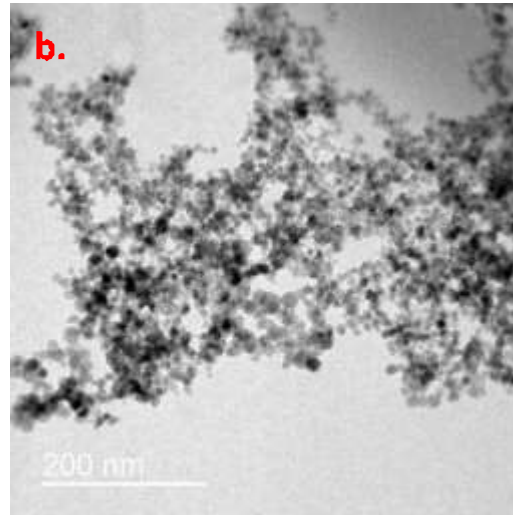
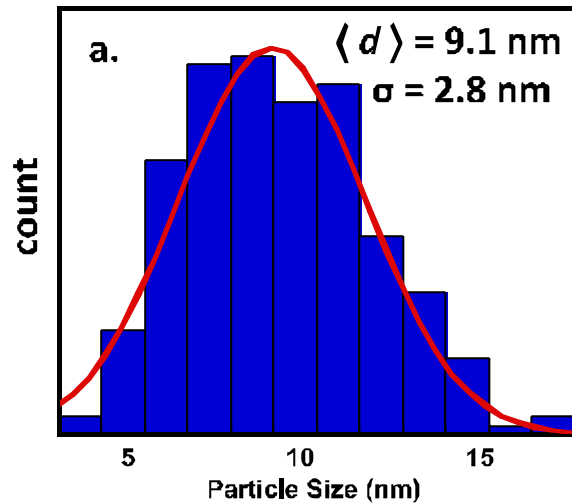
Flame	ϕ	T_{ad} [K]	$x_{\text{O}_2,eq}$	Crystallite size [nm] ^[a]	%(wt) anatase ^[b]
OR1	0.44	2385	1.8×10^{-1}	< 5	78
OR2	0.46	2329	1.5×10^{-1}	11.3	93
OR3	0.59	2667	1.5×10^{-1}	17.7	94
OL1	1.19	2557	3.3×10^{-3}	< 5	30
OL2	1.15	2560	4.4×10^{-3}	7.5	26
OL3	1.33	2606	1.7×10^{-3}	12.1	29
1a ^c	0.52	2354	1.3×10^{-1}	11	91
1b ^c	0.68	2551	8.5×10^{-2}	13	95
1c ^c	0.83	2652	5.4×10^{-2}	13	71
2a ^c	0.90	2651	3.7×10^{-2}	11	98
3a ^c	1.13	2782	1.6×10^{-2}	8	20
4a ^c	1.27	2797	9.3×10^{-3}	9	12

[a] as determined by XRD. [b] the balance is rutile. [c] taken from Memarzadeh et al.^[27]

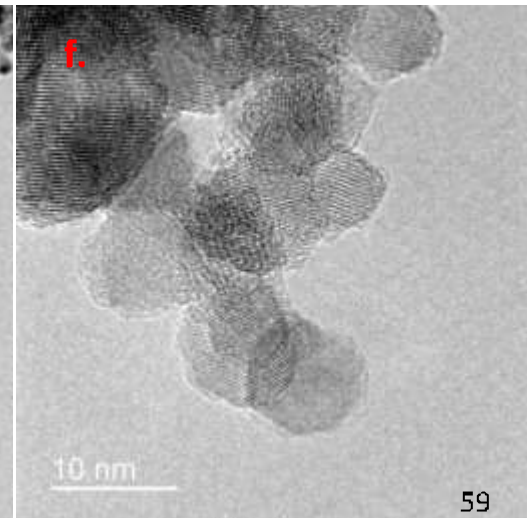
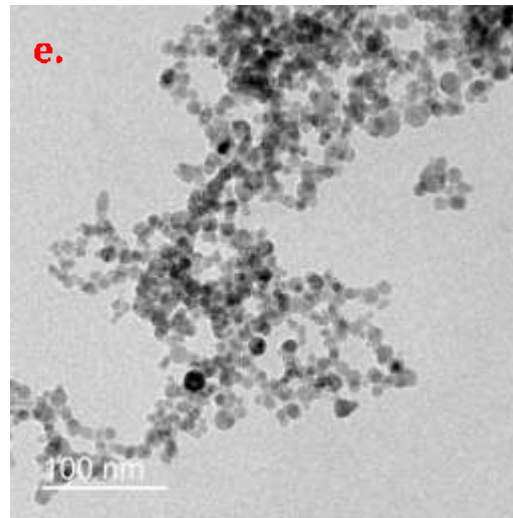
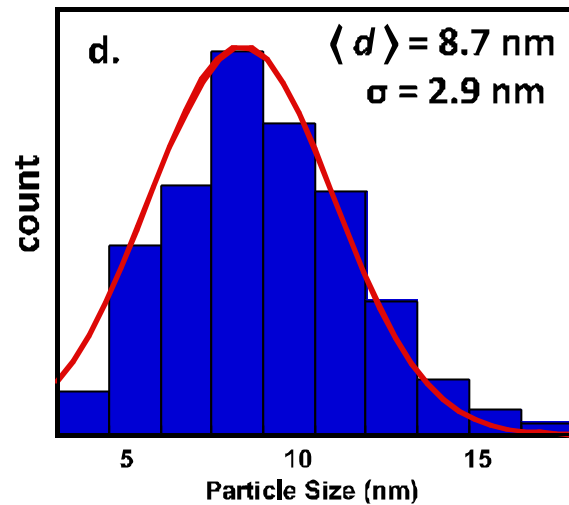


No Notable Differences in the Morphology or Size

Oxygen rich



Oxygen lean



TiO₂ Particle Surface Energy

Surface free energy of Rutile and Anatase:

$$\gamma_{R/Ti} = \underbrace{n_{s^-} \gamma_{Ti}}_{\text{O vacancies}} + \underbrace{(1 - n_{s^-}) \gamma_R}_{\text{Rutile Ti-O surface sites}} \quad \gamma_{A/Ti} = \underbrace{n_{s^-} \gamma_{Ti}}_{\text{O vacancies}} + \underbrace{(1 - n_{s^-}) \gamma_A}_{\text{Anatase Ti-O surface sites}}$$

Phase transition Gibbs free energy: $\Delta G^0 = \Delta G^0(r, T, X_{O_2})$

$$\Delta G^0 = \Delta_f G^0(T, \text{rutile}) - \Delta_f G^0(T, \text{anatase}) + (2t + 3) \frac{M}{r} \left(\frac{\gamma_{R/Ti}}{\rho_R} - \frac{\gamma_{A/Ti}}{\rho_A} \right)$$

Determine Surface Vacancy

Surface vacant site density: $n_{s^-} = \frac{\sqrt{K_p / X_{O_2}}}{1 + \sqrt{K_p / X_{O_2}}}$

Equilibrium constant: $K_p = \frac{(P_{(O_2)} / P_0) n_{s^-}^2}{(1 - n_{s^-})^2} = e^{-\Delta G^\circ / RT}$

Free energy of reaction: $\Delta G^\circ = \Delta H_r - T \Delta S^\circ$

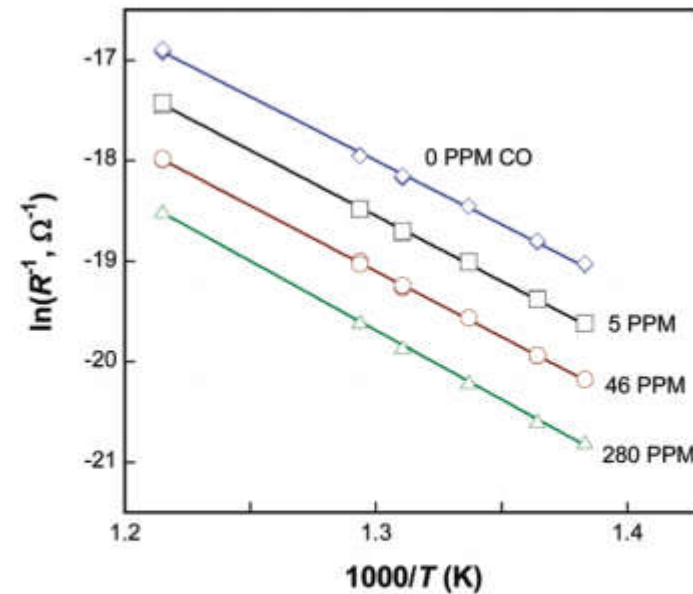
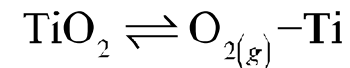
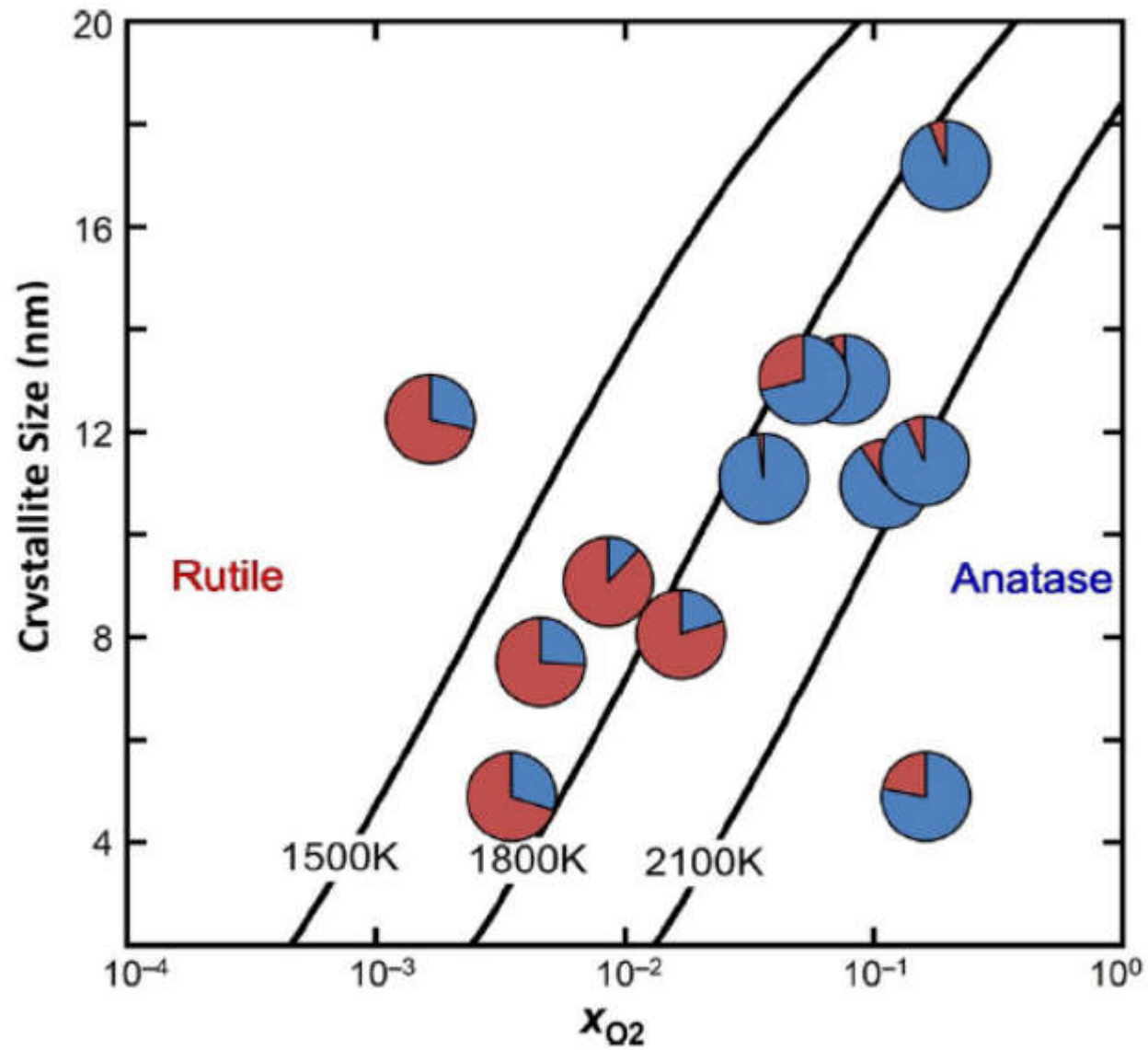


Figure 11. Pseudo Arrhenius plot of conductance of the FSRS-2 sensor film. The apparent activation energy is $E_a = 25.2 \pm 0.2$, 25.9 ± 0.2 , 25.9 ± 0.2 , and 27.4 ± 0.3 kcal/mol for 0, 5, 46, and 280 PPM CO, respectively.

New TiO₂ Phase Diagram with surface desorption equilibrium



Concluding Remarks

- On one level there is value in creating models of soot formation as an integral part of engine design codes, but the largest impact perhaps will be to apply what we have learned about soot formation in flames to many different prospects of nanoparticle synthesis.
- The greatest benefits of current knowledge will lie not in incremental improvements in soot reduction but in creating particles of value in energy, catalysis and yet unimagined fields.